

Milagro Collaboration



Contributions to

XXVIth ICRC Salt Lake City, UT

August, 1999

Status of the Milagro Gamma Ray Observatory

J.F. McCullough¹ for the Milagro Collaboration

¹*Department of Physics, University of California, Santa Cruz, CA 95056, USA*

Abstract

The Milagro Gamma Ray Observatory is the world's first large-area water Cherenkov detector capable of continuously monitoring the sky at TeV energies. Located in the mountains of northern New Mexico, Milagro will perform an all sky survey of the Northern Hemisphere at energies between ~ 250 GeV and 50 TeV. With a high duty-cycle ($\sim 100\%$), large detector area (~ 5000 m²), and wide field-of-view (~ 1 sr), Milagro is uniquely capable of searching for transient and DC sources of high-energy γ -ray emission. Milagro has been operating since February, 1999. The current status of the Milagro Observatory and initial results will be discussed.

1 Introduction

Observations in high-energy γ -ray astronomy can be performed with either satellite or ground-based detectors. Satellite-based telescopes directly detect photons by converting them and then tracking the electron-positron pairs. Ground-based telescopes detect the secondary charged particles in the extensive air shower (EAS) that results when an incoming photon interacts with the earth's atmosphere. Because of the low fluxes involved in high-energy γ -ray astronomy and the relatively small detectors that can be placed on satellites, observations above a few 10s of GeV must be performed from the ground.

Atmospheric Cherenkov telescopes (ACTs) have been used with great success in the energy region from ~ 300 GeV - 10 TeV. ACTs detect the Cherenkov radiation produced in the atmosphere from the relativistic charged secondaries in an EAS. The advantages of ACTs over other ground-based techniques is that they have a low energy threshold, very good angular resolution and excellent background rejection capabilities. However, ACTs are pointed telescopes with a small field of view and can therefore only observe one source at a time. In addition, because they are optical instruments, ACTs have a very small duty factor ($\sim 10\%$) since they can only be used on clear, dark nights.

In the energy region above ~ 40 TeV, enough secondary particles from an EAS reach the ground that an extensive air-shower particle detector array can be used. This typically consists of a sparse array of scintillation counters that detect the charged particles from an air shower that reach ground level. EAS arrays can observe the entire overhead sky at once and can therefore observe all sources within their field of view simultaneously. They can also be operated 24 hours a day in all weather conditions. However, EAS arrays typically cover only $< 1\%$ of the ground with detectors and therefore only detect a small fraction of the charged particles reaching the earth's surface. Because of this, EAS arrays have a much higher energy threshold than ACTs and have very limited background rejection capabilities.

Ideally, one would like to have the high duty factor and large aperture of EAS arrays in the energy region covered by ACTs. This would allow the first all-sky survey to be done at TeV energies. In order to accomplish this with an EAS array, one could move to a higher altitude, detect a larger fraction of the charged particles reaching ground level, or increase the sensitivity to the photons from the EAS that reach the ground. Milagro has incorporated the last two ideas to achieve an energy threshold of ~ 250 GeV while maintaining a high duty factor and large aperture.

2 Detector Design

Milagro is the first large-area water-Cherenkov detector specifically built to study extensive air showers. The detector is located in the mountains of northern New Mexico at an altitude of 2650m. Milagro is built in a

man-made pond formerly used as part of a geothermal energy project. The pond is $60 \times 80 \text{ m}^2$ at the surface and has sloping sides that lead to a $30 \times 50 \text{ m}^2$ bottom at a depth of 8 m. It is filled with 5 million gallons of purified water and is covered by a light-tight high-density polypropylene liner. Milagro consists of two layers of upward pointing 8" diameter hemispherical Hamamatsu 10-stage photomultiplier tubes (PMTs). Each PMT is lifted by its buoyant force (~ 8 pounds each) and is anchored by Kevlar strings to a $3 \times 3 \text{ m}^2$ support grid of 3" PVC pipe filled with wet sand. The top (air-shower) layer of 450 PMTs is located 1.4 m below the water's surface. This layer is used to trigger the detector and measure the arrival time of the air-shower wave front. The second (hadron/muon) layer consists of 273 PMTs located at a depth of approximately 7 m. The hadron layer is used to make a calorimetric measurement of the shower, to differentiate γ -induced air showers from cosmic-ray induced showers and to detect muons.

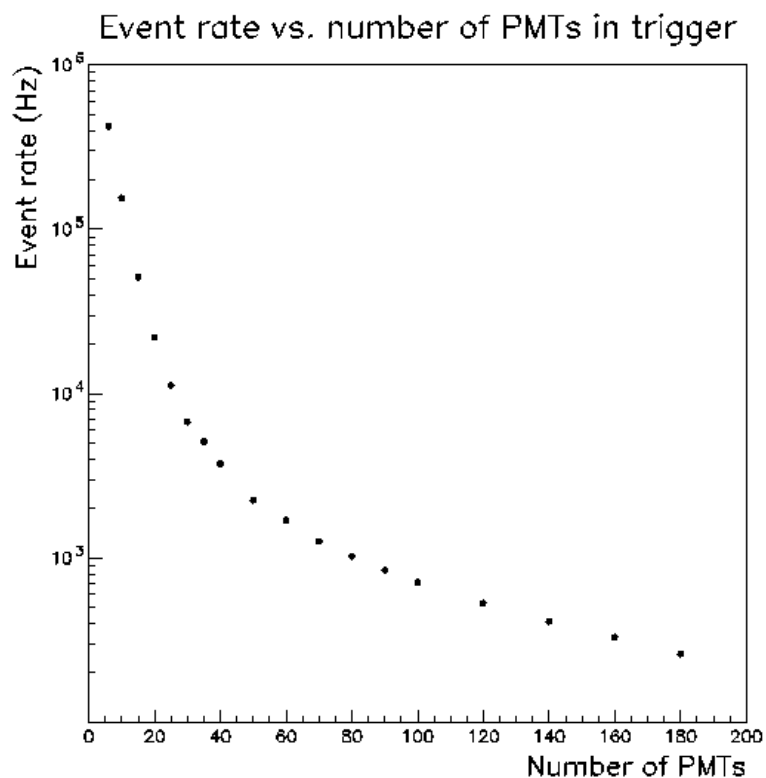


Figure 1: Event rate vs. number of PMTs required to trigger the detector

The use of water as a detection medium has several distinct advantages over EAS arrays that employ scintillation counters. At the earth's surface, there are 4-5 times more photons in an extensive air shower than charged particles. When these photons enter the water, they convert to electron-positron pairs or Compton scatter electrons; these products are subsequently detected by the Cherenkov radiation that they emit. Since the Cherenkov light cone in water is large ($\sim 42^\circ$), the radiation spreads out so that a sparse array of PMTs provides complete coverage of the entire pond. Milagro therefore provides nearly 100% coverage of the surface as compared to $< 1\%$ for a scintillation array. The increased sensitivity to photons and the detection of a greater fraction of the charged particles in an EAS allows Milagro to achieve a substantially lower energy threshold than scintillation arrays.

3 Event Reconstruction

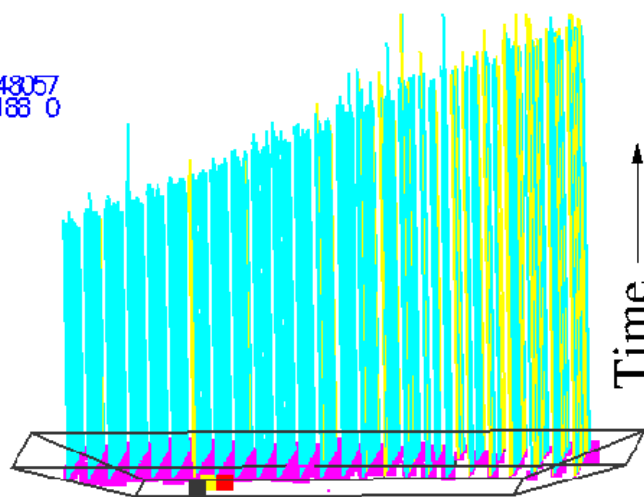
The trigger condition currently used is a simple multiplicity of PMT hits within a coincidence window of approximately 200 ns. Figure 1. shows the event rate for Milagro as a function of the number of air-shower PMTs required to trigger the detector. For each event, the arrival time and pulse height (number of photoelectrons or PEs) for each PMT hit are recorded. From this information, a number of quantities including the direction of the incident primary, the location of the shower core, and the energy of the primary particle are reconstructed. Of these quantities, the direction of the primary is the most important since the detection of a γ -ray source is based primarily upon the observation of an excess of events above the isotropic background of cosmic-ray induced air showers from a particular region of the sky.

To determine the direction of the primary γ -ray (or cosmic-ray), Milagro employs the same technique used by conventional scintillation-counter arrays. After the primary γ -ray or cosmic-ray interacts in the atmosphere and creates an air shower, the secondary particles are all highly relativistic and therefore beamed forward in the

direction of the primary. The end result (to a first approximation) is a flat pancake, perpendicular to the incident γ -ray or cosmic-ray, composed of many thousands of photons, electrons, positrons, and hadrons traveling parallel to the direction of the primary particle. By measuring the relative times that PMTs in the air-shower layer are struck by the Cherenkov radiation, the direction of the primary particle is reconstructed. An example of a reconstructed shower in Milagro is shown in Figure 2. The orientation of the fitted plane is determined by a least-squares (χ^2) fit to a more complex shower-front shape using the measured times and positions of the air-shower PMTs. The angular resolution of Milagro depends upon the number of PMTs used in the fit. Monte Carlo simulations of the detector response suggest a typical angular resolution of less than 1° .

```
Event No 10
Julian Day 1277
Seconds 25662548057
N PMTs : 381 188 0
```

```
Fit Information (asmuon):
Theta 34.74 37.06 34.74
Phi 101.24 96.70 101.24
ChiSq 3.16 1.530
N Fit 163 55
```



Milagro event - air shower layer

Figure 2: Event display for Milagro. Vertical lines are proportional to the arrival time

The location of the shower core and the energy of the primary particle are reconstructed from the amplitudes and distributions of pulse heights of hit PMTs in both the air shower and hadron layers. The ability to reconstruct the energy of the primary depends heavily on the ability to find the shower core. This is because a high energy shower hitting far from the pond and a low energy shower hitting close to the pond can both appear the same to Milagro, which only has information on the particles entering the water. To allow a better determination of the core location for showers which land outside the pond, a sparse array of water tanks is being deployed around Milagro. Each water tank is equipped with a PMT that detects most of the shower particles entering it. Monte Carlo simulations predict that with an array of 172 water tanks, Milagro will be able to find the shower core to within approximately 15 meters (Shoup et al., 1999).

Background rejection is accomplished using the pulse heights of the hadron layer PMTs. Muons penetrating to the hadron/muon layer leave a very distinct signal as can be seen in Figure 3. One or two PMTs are usually hit with amplitudes ≥ 20 photo-electrons while the neighboring tubes have much lower amplitudes. Since muons are mainly produced in cosmic-ray induced air showers, any event identified as containing a muon is thrown out. We thus have an effective method of background rejection. One disadvantage with this method is that it only works if a muon strikes the pond. According to Monte Carlo simulations, this only happens in approximately 50% of the proton showers which trigger Milagro. Other algorithms for identifying background events based on the distribution of light in the hadron/muon layer are promising and are currently being investigated.

4 Milagro Operation and Results

A prototype detector (Milagrino) was operated from February 1997 to May 1998. Milagrino was approximately half the size of Milagro ($\sim 2500 \text{ m}^2$) and consisted of a single layer of 228 PMTs. Data was

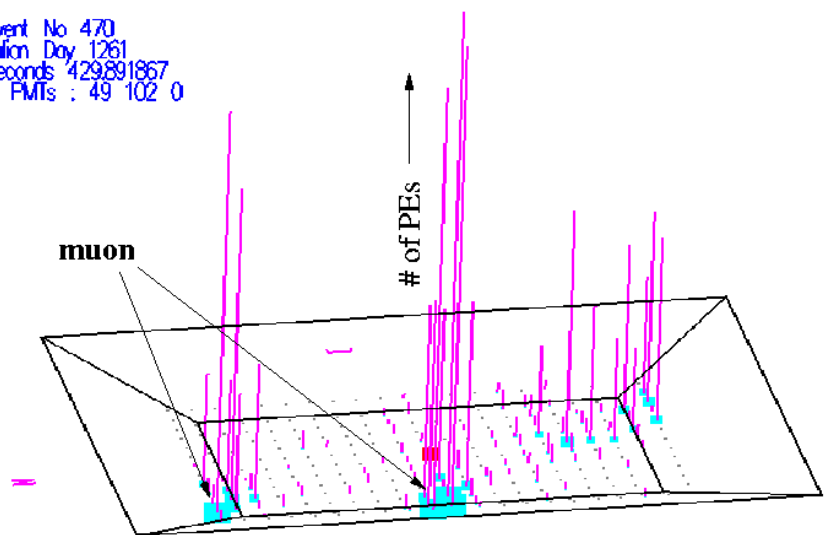
taken with the PMTs at depths of 1.0m, 1.5m, and 2.0m to determine the effect of water depth on angular resolution. Because Milagrito had only one shallow layer of PMTs, it had very limited background rejection. The angular resolution for Milagrito was $\sim 1^\circ$. Milagrito used a trigger condition of 100 PMTs hit within a coincidence window of 300ns. This resulted in an event rate of 300-400 Hz, depending on the water depth. In the 15 months of operation of Milagrito, we collected $\sim 8.9 \times 10^9$ events and wrote ~ 9 Terabytes of data to tape.

Although Milagrito was operated mainly as a test run for this relatively new water-Cherenkov technique, it was a fully operational detector that has produced

several interesting scientific results. Milagrito detected the moon shadow with a significance of 10σ (Wascko et al., 1999), detected Markarian 501 with a significance of $> 3\sigma$ (Westerhoff et al., 1999), and detected the Nov. 6, 1997 solar coronal mass ejection (Ryan et al., 1999). We are continuing to analyze the Milagrito data.

Milagro was installed in the summer of 1998 and began taking data in February 1999. The electronics for Milagro use the same time-over-threshold technique used in Milagrito (Atkins et al., 1999). As of this writing, Milagro is in an engineering mode. The PMTs are being calibrated and final adjustments to the data acquisition system are being made. The Milagro trigger is currently 150 PMTs hit within 200ns. This results in an event rate of ~ 350 events per second and ~ 75 Gigabytes of data written to tape each day. We have collected ~ 2 billion events to date. We expect to begin normal operations in early June. Preliminary results from the Milagro data will be presented at the conference.

Event No 470
 Julian Day 1261
 Seconds 429.891867
 N PMTs : 49 102 0



Milagro event - hadron layer

Figure 3: Event display for Milagro. Vertical lines are proportional to pulse height

Acknowledgements

This research is supported in part by the National Science Foundation, the U.S. Department of Energy Office of High Energy Physics, the U.S. Department of Energy Office of Nuclear Physics, Los Alamos National Laboratory, the University of California, the Institute of Geophysics and Planetary Physics, The Research Corporation, and the California Space Institute.

References

- Atkins et al. 1999, Nucl. Instr. Meth. A , in preparation
- Ryan, J. et al. 1999, Proc. 26th ICRC (Salt Lake City, 1999) SH 1.7.02.
- Shoup, A. et al. 1999, Proc. 26th ICRC (Salt Lake City, 1999) OG 4.4.06.
- Wascko, M.O. et al. 1999, Proc. 26th ICRC (Salt Lake City, 1999) SH 3.2.39.
- Westerhoff, S. et al. 1999, Proc. 26th ICRC (Salt Lake City, 1999), OG 2.1.11.

Single hadrons in Milagro and the Spectrum of Cosmic Ray Protons

Gaurang B. Yodh¹, for the Milagro Collaboration

¹*Department of Physics and Astronomy, University of California, Irvine, CA, 92697*

Abstract

Single unaccompanied hadrons can be used to probe the shape and intensity of the primary cosmic ray proton spectrum. The Milagro detector can be used as a very large calorimeter with an effective area of 2000 m² and a thickness of 7 meters (7 interaction lengths and 15 radiation lengths) to sample primary protons which survive to Milagro level without interacting in the atmosphere. The response of the shower layer (PMTs located below about 2 meters of water) is used to establish calorimeter penetration by single unaccompanied hadrons and the hadron energy measured from the response of the PMTs located below 7 meters of water. A data set from three years of operation can be used to establish the presence of a bend in the proton spectrum if it is below 500 TeV. Results from simulation, which illustrate the method, and some preliminary experimental results showing feasibility using data from Milagrito will be presented.

1 Principle of the Technique:

At high energies (energies above a few TeV) most cosmic rays produce air showers at the Milagro altitude of 750 gm/cm². Energetic hadrons in the shower which retain a significant fraction of the energy of the incident cosmic ray are located within few meters of the core of the shower. A fraction $\exp(-\frac{x}{\lambda(E)})$ will survive without any interaction in slant depth x and they will not have a shower associated with them. The interaction length $\lambda(E)$ for proton air inelastic cross sections can be calculated from a knowledge of the p-p total cross section and the elastic slope parameter using Glauber techniques (Gaisser et al., 1987). A measurement of the energy spectrum of the surviving hadron flux can be used to estimate the energy spectrum of primary protons and search for a possible cut-off in the spectrum above 100 TeV which has so far eluded detection (Swordy, 1993).

As the fraction of surviving hadrons is small ($\sim 10^{-4}$), a very large and reasonably deep calorimeter to detect these hadrons and measure their energies is required. In addition, events with accompanying shower particles must be rejected. The Milagro TeV gamma ray telescope satisfies these requirements. Its bottom layer, which is about 2000 m² in area and whose PMTs can collect the Cherenkov light produced by the cascade produced by energetic hadrons in about 7 meters depth of water ($7 \lambda_{int}$ and $15 \lambda_{rad}$) can be considered a calorimeter to measure energetic surviving hadrons and its top layer can be used to ensure lack of shower accompaniment.

The experiment measures an upper limit to the primary flux of cosmic ray protons. This upper limit approaches the true flux as energy increases because the probability of rejection of events with small accompaniment increases with energy. Thus contamination from events with accompaniment will make the estimated proton spectrum steeper than the true spectrum at low energies (below a TeV) and then at higher energies (greater than 10 TeV) the spectral slope would more accurately reflect the true slope of primary protons. A cutoff in the primary proton spectrum above 100 TeV should manifest itself as a steepening in the slope of the measured spectrum. The contribution to this unaccompanied flux from higher A nuclei can be shown to be small at these high energies.

2 Estimate of Number of Events:

The expected event rate can be estimated using measured values of the primary proton flux and calculated values of the proton-air inelastic cross section as a function of energy. Most of the single hadron flux comes from near zenith. For this calculation protons and alpha primaries were both included. Figure 1 shows integral spectrum of expected number of events of surviving hadrons for a 3000 m² area calorimeter. Two sets of points

are shown corresponding to no steepening of the primary cosmic ray proton spectrum up to the knee, ~ 1 PeV (designated no cutoff) and to a steepening of the spectrum at 100 TeV with an increase in spectral slope of 0.5 (designated cut off). These numbers are also consistent with previously measured fluxes of unaccompanied particles at mountain level (Siohan78). The integral spectra for single hadrons in Milagro with an area of 2000 m^2 and an operation time of 3 years, corresponds to collecting 400 events above 60 TeV with no cut-off, and only 290 events above the same energy with a cut-off at 100 TeV. A steepening of slope in the surviving hadron spectrum would be observable, indicating a steepening of the spectrum of primary protons in cosmic rays.

In addition to events attributable to single hadrons, high energy muons can produce cascades due to catastrophic energy loss, such as muon bremsstrahlung. This contribution can be shown to be less than a few percent of the single hadron rate and the zenith angle distribution of events due to muons will be much flatter than that of single hadrons. The muon generated events can be estimated from observed zenith angle distribution of cascades.

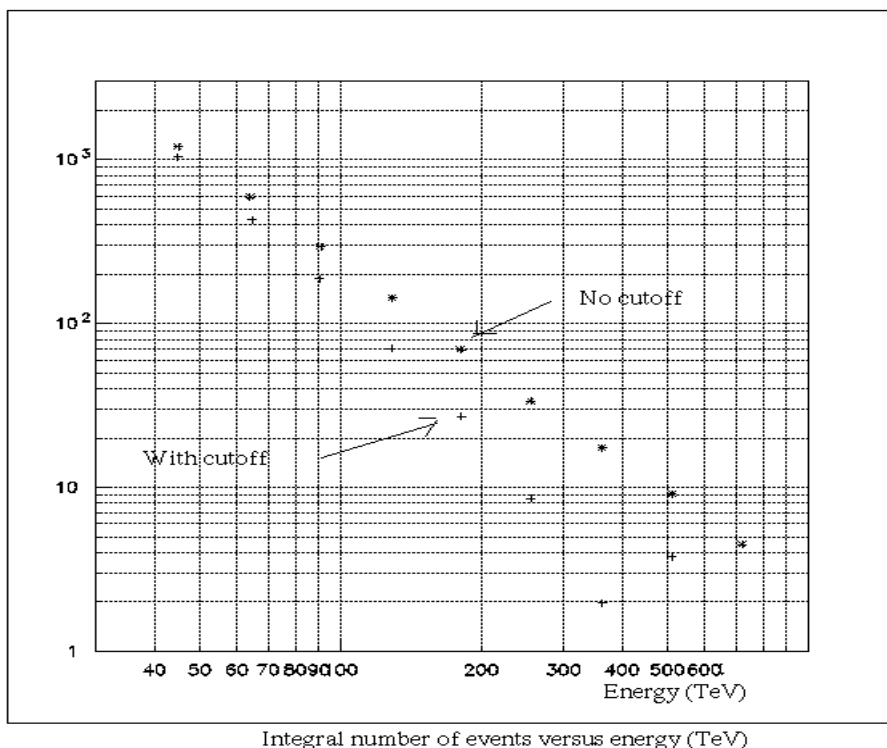


Figure 1: Integral spectrum for number of events expected for a 3000 m^2 detector in three years. Ordinate is $N(\geq E)$

3 Some Results from Milagrito:

The Milagrito detector, which was a one layer Milagro prototype with 1.5 m of water above PMTs, operated for about a year. We made a preliminary search for single hadrons in Milagrito. Single hadrons should produce a large quantity of localized light in the region of the cascade developed by the energetic hadron. Simulation of single hadron cascades shows that in addition to localized large pulse-heights near the core of the cascade, a large number of other PMTs were lit up with low pulseheights from light produced by particles in the cascade due to multiple scattering of low energy electrons in the cascade. A study of timing distributions of these lit tubes with respect to the timing of the largest tube showed time delay of these hits to be what would be expected for light travelling at the speed of light in water. In a plot of time versus position of each tube with respect to the hottest tube can be fitted with a straight line which corresponds to speed of light in water. An

example of this behaviour on a time versus distance scatter plot for 1 TeV simulated single hadron events is shown in Figure 2. Single hadrons were selected from Milagrito data by requiring that 90 percent of all hits lie in a band around the speed of light in water line. A relatively clean sample of single hadrons was obtained. Figure 3 shows a lego plot of a selected single hadron event selected using the cut on delay times. The figure shows pulse heights in terms of equivalent number of photo-electrons (pes) for each tube(z axis) and (x,y) location of the tube. The figure clearly shows a localized cascade due to the energetic hadron.

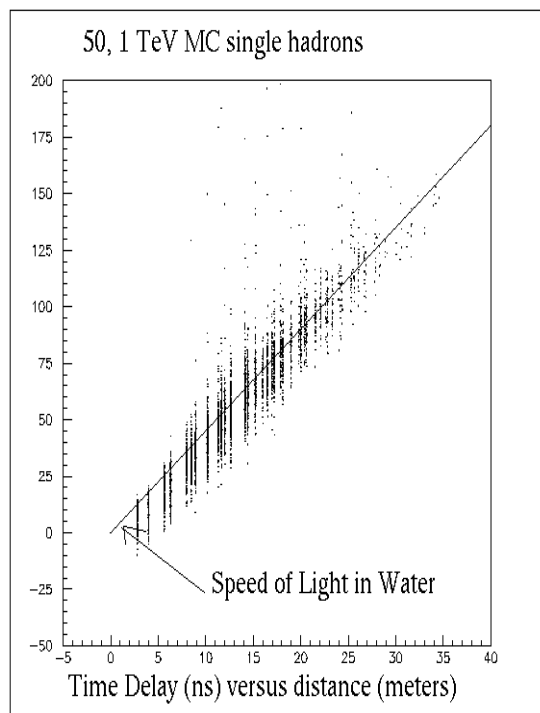


Figure:2 Time delay(x) versus distance from the high-pulse height tube(y), for 1 TeV MC protons. The line represents speed of light in water.

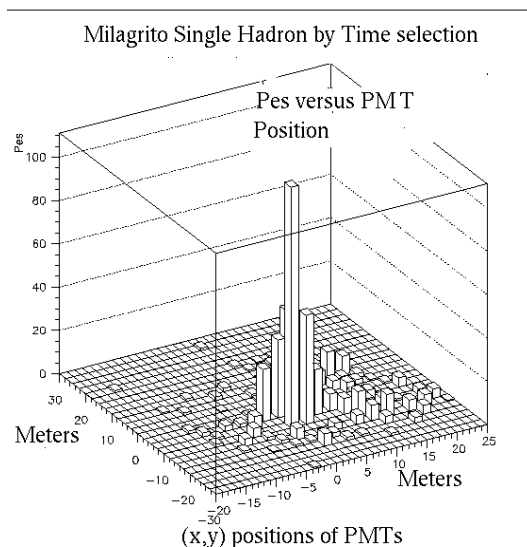


Figure 3: A typical single hadron selected from data. Lego plot of pulse heights

The observed photo-electron(pes) spectrum for single hadrons selected from data by the technique described above is compared with that obtained from simulation in Figure 4. The x axis is the logarithm of the total number of pes detected in Milagrito. The simulation imposed the same trigger cuts as the data and generated events for surviving hadrons from cosmic ray protons with a threshold well below trigger level and on a spectrum with slope of -2.7. The reasonable similarity between the shapes of these two distributions indicates that the criteria for picking out single hadrons works. The number of total pes in the current simulation have about a systematic uncertainty of 30 percent. Further work is in progress to minimize this uncertainty.

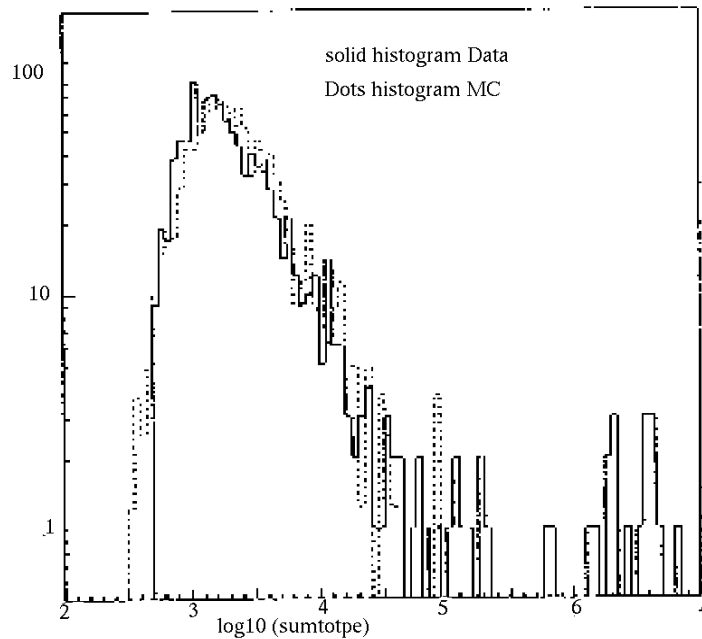


Figure 4: Comparison of MC and Data single had spectra
Solid histogram is data and dashed is MC

4 Concluding Remarks

Milagro has just begun operation. We will study the data to determine the best method to pick out triggers due to single hadrons in Milagro and also develop special triggers to select single hadrons. This study of single hadrons should complement the composition studies we plan to do using a Wide Angle Cherenkov Telescope(WACT) array (Atkins99).

This work is supported in part by National Science Foundation, U.S. Department of Energy Offices of High Energy Physics and Nuclear Physics, the University of California, Los Alamos National Laboratory, the U.C. Institute of Geophysics and Planetary Physics, the Research Corporation and the California Space Institute.

References

- Atkins R., et al., 1999, Proc. 26th ICRC (Utah), paper O.G.4.3.34
- Gaisser, T. K., Sukhatme, U.P.,& Yodh, G. B., 1987, Phys. Rev. D36, 1350.
- Siohan, F, et. al.,1978, J. Phys. G, Nuclear, 4, 1169.
- Swordy, S. , 1993, Proc. 23rd ICRC (Calgary), World Scientific,ed, D.A. Leahy, R. B. Hicks and D. Venkatesan, p243.

Milagrito Detection of TeV Emission from Mrk 501

Stefan Westerhoff¹ for the Milagro Collaboration

¹University of California, Santa Cruz, CA 95064, USA

Abstract

The Milagro water Cherenkov detector near Los Alamos, New Mexico, has been operated as a sky monitor at energies of a few TeV between February 1997 and April 1998. Serving as a test run for the full Milagro detector, Milagrito has taken data during the strong and long-lasting 1997 flare of Mrk 501. We present results from the analysis of Mrk 501 and compare excess and background rate with expectations from the detector simulation.

1 Introduction:

With the detection of 4 Galactic and 3 extragalactic sources, Very High Energy (VHE) γ -ray astronomy, studying the sky at energies above 100 GeV, has become one of the most interesting frontiers in astronomy. Source detections and analyses in this field are still dominated by the highly successful atmospheric Cherenkov technique. Cherenkov telescopes and telescope arrays are optimal tools for the detailed study of established sources and their energy spectra and the theory-guided search for yet unknown sources. There is, however, also a strong case for instruments able to perform an unbiased, systematic and continuous search for TeV sources, thus overcoming the limitations imposed by the low duty cycle and small field of view of Cherenkov telescopes. Consequently, the observation technique must exploit the *particle content* of air showers rather than the Cherenkov light.

A first-generation all-sky monitor operating at energies below 1 TeV, the Milagro detector (McCullough et al., 1999) located 2650 m above sea level near Los Alamos, New Mexico, at latitude $\lambda = 35.9^\circ$ N, started data taking in early 1999. Milagro is a water Cherenkov detector of size $60 \times 80 \times 8 \text{ m}^3$. Two layers of photomultiplier tubes detect the Cherenkov light produced by secondary particles entering the water. The first layer, with 450 tubes on a $3 \times 3 \text{ m}^2$ grid at a depth of 1.4 m, allows the shower direction and thus the direction of the primary particle to be reconstructed, while the second layer with 273 tubes at a depth of ~ 7.0 m primarily detects the penetrating component of air showers, *i.e.* muons, hadrons, and highly energetic electromagnetic particles.

A smaller, less sensitive prototype, Milagrito (Atkins et al., 1999), has taken data between February 1997 and April 1998. Milagrito, a one-layer detector of size $35 \times 55 \times 2 \text{ m}^3$ with 228 photomultiplier tubes on a $3 \times 3 \text{ m}^2$ grid at a rather shallow depth of 0.9 m, served mainly as a test run for this relatively new detection technique. This prototype has, however, taken data during a very intense and long-lasting flare of Mrk 501 in 1997 (Samuelson et al., 1998).

For the evaluation of the performance of VHE instruments, the Crab nebula is usually used as a “standard candle”. It is a well-studied steady source with a flux of

$$J_\gamma(E) = (3.20 \pm 0.17 \pm 0.6) \times 10^{-7} E_{\text{TeV}}^{-2.49 \pm 0.06 \pm 0.04} \text{ m}^{-2} \text{ s}^{-1} \text{ TeV}^{-1}, \quad (1)$$

(Hillas et al., 1998). Simulations indicate that the expected significance from Milagrito for the Crab nebula is less than 2σ , ruling out the possibility of using a Crab signal to test Milagrito’s performance. A detection of Mrk 501 with a sufficiently high significance can be expected had the average flux been in excess of the Crab flux. During its flare in 1997, Mrk 501 has been intensively studied with several air Cherenkov telescopes. Although not covering the same observation times, the average fluxes measured by Whipple (Samuelson et al., 1998) and the HEGRA stereo system of air Cherenkov telescopes (Aharonian et al., 1999) agree extremely well both in shape and magnitude, and they both indicate a significant deviation of the energy spectrum from

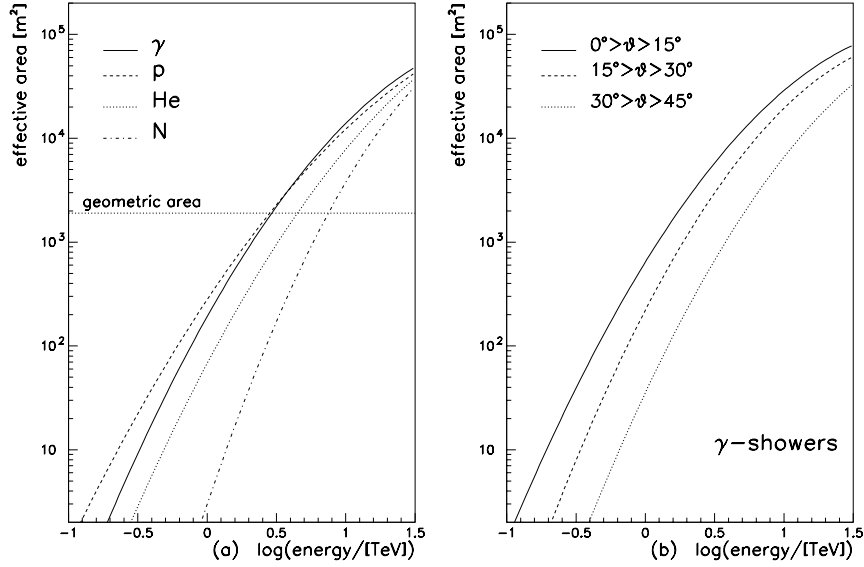


Figure 1: (a) Effective area of Milagrito for reconstructed γ - and cosmic ray showers, averaged over a zenith angle range from $0^\circ \leq \theta \leq 45^\circ$, as a function of the primary energy. (b) Effective area for γ -showers for various zenith angle ranges.

a simple power law. Using an average flux as measured by Whipple,

$$J_\gamma(E) = (8.6 \pm 0.3 \pm 0.7) \times 10^{-7} E_{\text{TeV}}^{-2.20 \pm 0.04 \pm 0.05 - (0.45 \pm 0.07) \log_{10} E} \text{ m}^{-2} \text{ s}^{-1} \text{ TeV}^{-1}, \quad (2)$$

simulations of the Milagrito detector response predict the expected integral γ -rate from Mrk 501 to be 3.6 times the Crab rate. Although highly variable sources like Mrk 501 are not well-suited for checking the sensitivity of detectors integrating over long time periods, the observation of an excess from Mrk 501 still provides a test for the sensitivity of Milagrito and reliability of the detector simulation.

In addition, observations with Cherenkov telescopes cover only the time from February to October, while Milagrito continued to monitor Mrk 501 in late 1997 and early 1998.

2 Milagrito Performance:

Sensitivity predictions for Milagrito are based on a detector simulation using the CORSIKA 5.61 air shower simulation code for the development of the shower in the Earth's atmosphere, and the GEANT 3.21 package for the simulation of the detector. The simulation is described in detail elsewhere (Atkins et al., 1999).

The Milagrito detector operated with a minimum requirement of 100 hit tubes per event. Figure 1 (a) shows the effective area A_{eff} of Milagrito for γ -showers and cosmic ray background showers induced by protons, helium, and nitrogen, the latter used for representing the combined CNO flux, as a function of the energy of the primary particle. Figure 1 (b) shows how the efficiency depends on the zenith angle θ .

At energies ≤ 2 TeV, the effective area for proton-induced showers is larger than for γ -showers. This is related to the fact that γ -induced (thus almost purely electromagnetic) showers are usually more laterally confined so the area covered by the particles reaching detector altitude is smaller than for hadron-induced showers, which tend to have "hot spots" with high particle density at large distances from the shower core. At energies above ~ 5 TeV, the larger effective area for γ -induced showers provides an intrinsic cosmic ray background rejection.

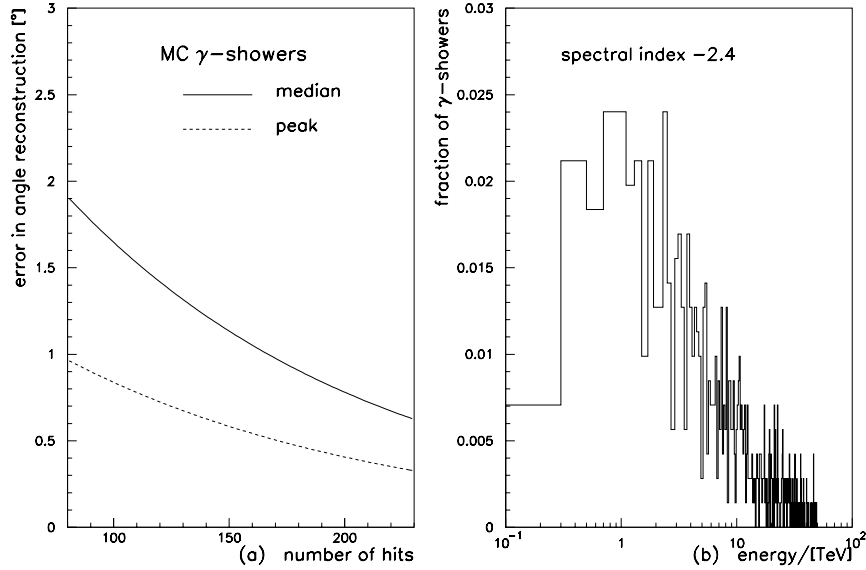


Figure 2: (a) Angular resolution and (b) energy distribution of γ -showers triggering Milagrito.

As a large fraction of showers fulfilling the trigger condition have their core outside the sensitive detector area, the effective area is larger than the geometrical area above ~ 3 TeV. In fact, only 16 % of the proton showers and 21 % of the γ -showers triggering the Milagrito detector have their core on the pond. This leads to a rather broad energy distribution starting at energies as low as 100 GeV, with no well defined threshold energy (Figure 2 (b)). The median energy varies slightly with the source declination δ , ranging from ~ 3 TeV for sources at $\delta = 40^\circ$ to 7 TeV for sources with $|\delta - \lambda| \simeq 20^\circ$.

The water Cherenkov technique uses water both as the converter and the detector medium. Consequently, the efficiency for detecting low energy air shower particles is very high, leading to a good sensitivity even for showers with primary energy below 1 TeV. The angle fitting, however, has to deal with a considerable amount of light late as compared to the shower front reaching the detector. The “late light” is partly produced by low energy particles which tend to trail the shower front. More important, however, is the horizontal light component resulting from the large Cherenkov angle in water (41°), multiple scattering, δ -rays, and scattering and reflection of Cherenkov light. The expected angular resolution for cosmic rays agrees with our observations of the cosmic ray shadow of the moon (Wascko et al., 1999).

Milagrito’s angular resolution is a strong function of the number of the tubes in the fit to the arrival times of the tubes (Figure 2 (a)). For the initial source search, a minimum number of 40 tubes used in the shower plane fit is required. This leads to a measured rate of 2950 ± 98 reconstructed events per day from cosmic ray showers in a typical source bin with 1.1° radius at the declination of Mrk 501. This is in good agreement with the predicted rate of 3080^{+205}_{-110} events per day from protons, Helium, and CNO nuclei. In the simulation, the contribution of He and CNO to the total trigger rate turns out to be 27 % and 4 %, respectively.

3 Results:

A straight-forward analysis with a source bin of radius 1.1° centered on Mrk 501 leads to an excess $> 3\sigma$. According to simulations this bin size contains 48 % of the source events and is optimal for an analysis treating all events equally. The corresponding excess rate averaged over the lifetime of Milagrito (370 equivalent source days for Mrk 501) is $(8.7 \pm 3.0) \text{ day}^{-1}$.

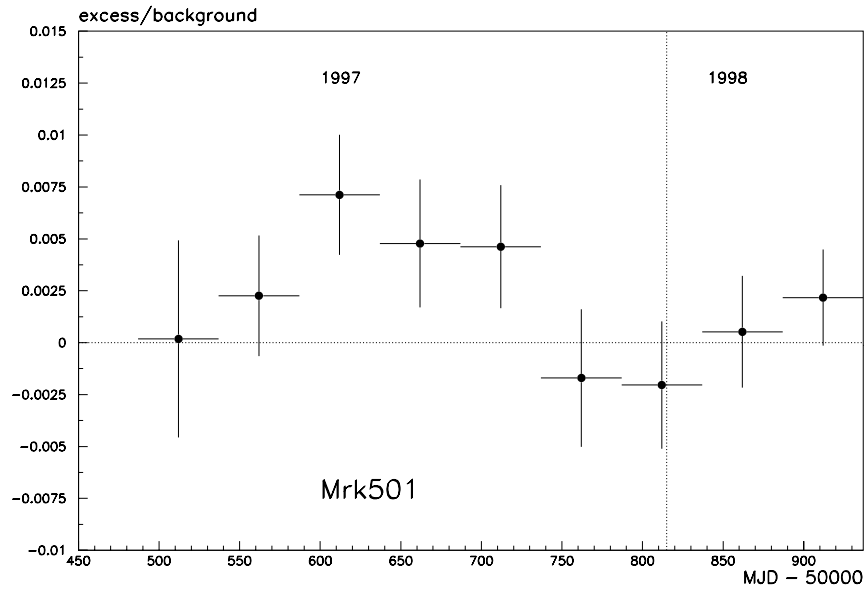


Figure 3: Excess/background for Mrk 501 as a function of time. At the current sensitivity level the data is consistent with a constant flux.

Figure 3 shows how the excess is accumulated over Milagrito's lifetime. At our present level of sensitivity, the data is consistent with a flux constant in time.

Using the average flux as measured by air Cherenkov telescopes between February and October 1997, simulations predict a γ -rate of $(13.3 \pm 4.0) \text{ day}^{-1}$ for Milagrito and are thus consistent with the measured excess during this period, $(15.3 \pm 4.6) \text{ day}^{-1}$.

An analysis that takes account of the strong dependence of the resolution on the number of photomultipliers in the fit should be more sensitive to emission from a point source. The results of such an analysis will be presented at the conference.

The analysis was extended to 10 other nearby blazars ($z \leq 0.06$) in Milagrito's field of view, but Mrk 501 remains the only analyzed source with a significance in excess of 3σ . Results from this blazar sample are reported elsewhere (Westerhoff et al., 1999).

This research was supported in part by the National Science Foundation, the U. S. Department of Energy Office of High Energy Physics, the U. S. Department of Energy Office of Nuclear Physics, Los Alamos National Laboratory, the University of California, the Institute of Geophysics and Planetary Physics, The Research Corporation, and the California Space Institute.

References

- Aharonian, F. et al. 1999, *Astron. & Astrophys.*, in press.
- Atkins et al. 1999, *Nucl. Instr. Meth. A*, in preparation.
- McCullough, J.F. et al., these ICRC proceedings (HE 6.1.02).
- Hillas, A.M. et al. 1998, *ApJ* 503, 744.
- Samuelson, F.W. et al., 1998, *ApJ* 501, L17.
- Wascko, M.O. et al., these ICRC proceedings (SH 3.2.39).
- Westerhoff, S. et al. 1999, *Proc. 19th Texas Symposium on Relativistic Astrophys.*, Paris (France), 1998.

Search for a TeV Component of GRBs Using the Milagrito Detector

Isabel R. Leonor¹ for the Milagro Collaboration

¹*Department of Physics and Astronomy, University of California at Irvine, Irvine, CA 92697, USA*

Abstract

Observing gamma ray bursts (GRBs) in the TeV energy range can be extremely valuable in providing insight to GRB radiation mechanisms and in constraining source distances. The Milagrito detector was an air shower array which used the water Cherenkov technique to search for TeV sources. Data from this detector was analyzed to look for a TeV component of GRBs coincident with low energy γ -rays detected by the BATSE instrument on the Compton Gamma Ray Observatory. A sample of 54 BATSE GRBs which were in the field of view of the Milagrito detector during its lifetime (February 1997 to May 1998) was used.

1 Introduction

Gamma ray bursts are the most electromagnetically luminous objects observed in the universe, releasing energies of 10^{51} - 10^{53} ergs in a few seconds in the form of γ -rays (Piran, 1999). Over the past two years, considerable progress was made in detecting optical and x-ray counterparts to GRBs, which has led to confirmation of their cosmological origin and has provided valuable insight into GRB energy conversion and radiation mechanisms. Before the advent of such lower energy detections, GRB emission was detected exclusively in the 10 keV to 18 GeV energy range by instruments such as those on the Compton Gamma Ray Observatory (CGRO) satellite, one of which is the Burst and Transient Source Experiment (BATSE). BATSE has been extremely successful in the detection and study of gamma ray bursts in the soft γ -ray energy range of 10 keV to 100 MeV. Operating since 1991, it has been detecting gamma ray bursts at the rate of about one burst per day.

In spite of these observations and recent progress in detecting counterparts, the origin of GRBs – which were first observed about 30 years ago – remains an enigma. Opening a new energy window for GRB observation in the TeV regime will be an invaluable aid in solving this mystery. Detection of TeV emission from GRBs will: (1) provide valuable information for modelling GRB radiation mechanisms; (2) constrain general quantitative properties of GRBs such as Lorentz factor and shock radius (Pilla & Loeb, 1998); (3) provide an upper limit to source distances owing to the predicted absorption of TeV gamma rays by intergalactic infrared (IR) photons; (4) contribute to the accurate determination of GRB locations and source identification. Current observations and GRB models do not rule out the existence of such higher energy component of GRBs. Indeed, it has long been asked if the lack of observed hard γ -rays from GRBs is due to observational bias and the lack of detectors suitable for such observations.

Non-detection of a TeV component, though leading to more ambiguous conclusions, will also have an impact since this will – if one assumes the existence of a TeV component – set a lower limit on the source distance scale and will provide evidence for gamma-ray absorption either at the source or by IR photons. Since gamma-ray fluxes at these high energies are very low, ground-based detectors such as Milagrito are the relevant instruments for detecting GRBs at the TeV regime.

The Milagrito detector (McCullough, et al., 1999) was an air shower array which used the water Cherenkov technique to detect TeV gamma-ray sources. It was located in the Jemez mountains of New Mexico, near Los Alamos, at an altitude of 2650 m above sea level. It consisted of 228 photomultiplier tubes (PMTs) in a light-tight pond of water. Arrival times at these PMTs of water Cherenkov light from air shower particles were used to reconstruct cosmic ray or γ -ray events incident on the atmosphere. It was operational from February 1997 to May 1998, detecting extensive air showers at a rate of 300-400 s^{-1} . Its angular resolution was typically $\sim 1.0^\circ$. With its large field of view, high duty cycle, and a sensitivity to γ -rays of ~ 1 TeV, Milagrito was a

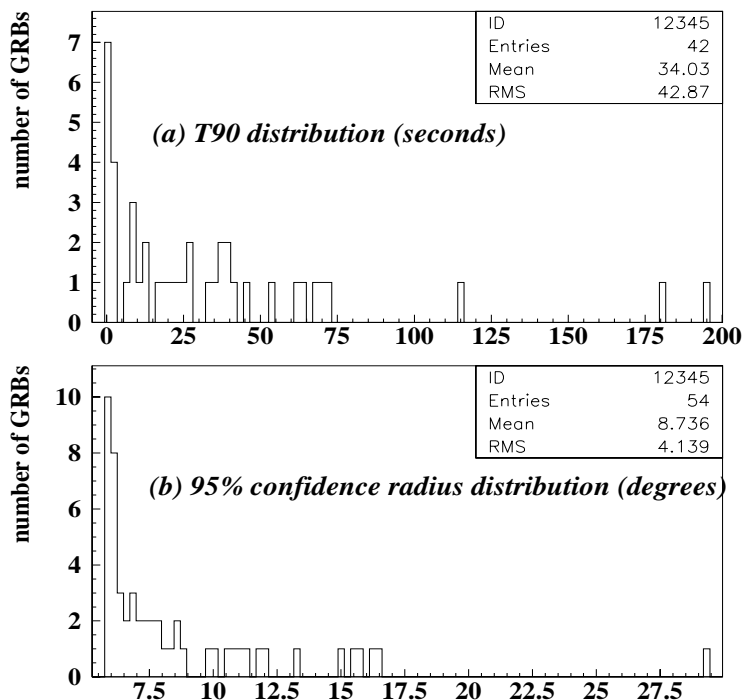


Figure 1: (a) T90 times and, (b) 95% confidence radii for the GRB sample.

practical instrument for observing gamma ray bursts which lasted but fleetingly and which were unpredictable in both time and position of occurrence.

During the Milagrito lifetime, 54 BATSE GRBs were within 45° of its zenith. Milagrito data was analyzed to look for evidence of emission of TeV γ -rays coincident with the low energy photons detected by BATSE from these GRBs. These GRBs are listed in Table 1. Of these 54 GRBs, there are 12 for which location arcs from the Third Interplanetary Network (IPN3) exist.

2 Method of Search

2.1 Search time duration and search area The search time duration used was T90, the time during which BATSE detected from 5% to 95% of the GRB counts. For the sample of 54 GRBs, this time ranged from hundreds of milliseconds to 200 seconds. The radius of the area used for the search was the 95% confidence radius for the BATSE GRB. This confidence radius is given as a function of the statistical error on the GRB position by the BATSE collaboration (Briggs, et al., 1999). The statistical error for the sample ranged from 0.6° to 18.0° , corresponding to 95% confidence radii of 6° to 29° .

Histograms of T90 times and 95% confidence radii are shown in Figures 1a and 1b.

The search area was covered by a grid of non-overlapping rectangular bins of equal areas on the celestial sphere, centered at the GRB (DEC,RA) position given by BATSE (see Figure 2). Optimal bin sizes were used in order to maximize the significance of a signal. These depend on the background count and Milagrito's angular resolution (Schnee, 1996). After this grid was searched, to ensure sensitivity to signals located near bin edges, the grid was shifted by half a bin width in DEC, then half a bin width in RA, then half a bin width in both. A search was done at each of these grid configurations, the end result being a search with overlapping, non-independent bins.

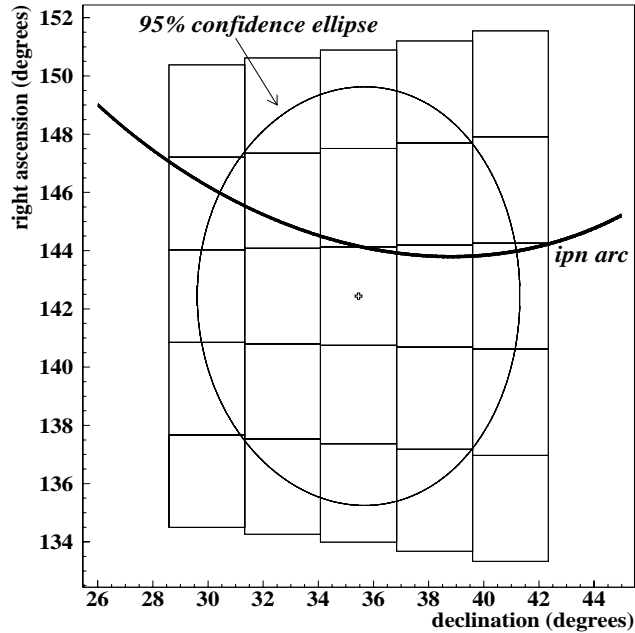


Figure 2: Search area and bin configuration for one GRB, showing the 95% confidence ellipse as well as the IPN3 arc. The center of the ellipse is the nominal GRB position given in the BATSE 4B catalog.

2.2 Background estimation Each (DEC,RA) bin of the search area at the middle of the T90 burst time interval (the assumed burst time) was mapped onto a corresponding local bin of the sky, (θ, ϕ) , and a careful measurement of the background count due to cosmic rays was made for each local (θ, ϕ) bin. Events occurring within a six-hour interval centered at the burst time, but excluding events occurring during the T90 burst interval, were put into time bins of duration T90 each. For each time bin, a different piece of the celestial sky was mapped onto the local sky. The events from each time bin falling into each local (θ, ϕ) bin were counted. The total number of events, $N_{off}(\theta, \phi)$, falling into a local bin (θ, ϕ) , divided by the total number of events, N_{tot} , coming from the entire sky, is the efficiency of the local bin (θ, ϕ) for detecting background events. The total number of events, N_{T90} occurring during the T90 search interval, and the total number of events, N_{2min} , occurring during a two-minute period centered at the middle of the burst search interval were also measured. The background estimate for the local (θ, ϕ) bin is then

$$B(\theta, \phi) = \frac{N_{off}(\theta, \phi)}{N_{tot}} N_{search} \quad (1)$$

where $N_{search} = (N_{2min}/120 \text{ s}) \times T90$ for $T90 < 120 \text{ s}$, and $N_{search} = N_{T90}$ for $T90 > 120 \text{ s}$. The use of N_{2min} is a safeguard against large uncertainties in N_{T90} when T90 is small. The background estimate in the form given by eq. (1) also ensures that rate changes occurring during the six-hour background period do not affect the background estimate for the search period.

2.3 Determining probabilities The number of events, $N_{on}(\text{DEC}, \text{RA})$, falling in each (DEC,RA) bin is measured and the Poisson probability for observing $N_{on}(\text{DEC}, \text{RA})$ events given an expected background of $B(\theta, \phi)$ at the local bin is calculated. Note that for the short search time intervals used in this analysis, the source was treated as if it did not move relative to the local sky.

3 Results

The results of this analysis, including significances of the measurements, will be presented at the conference.

BATSE trigger number	BATSE trigger date	BATSE fluence, E > 20 keV (ergs/cm ²)	Milagrito zenith angle	BATSE trigger number	BATSE trigger date	BATSE fluence, E > 20 keV (ergs/cm ²)	Milagrito zenith angle
6100	970223	7.85E-5	24.9°	6376	970910	2.10E-7	38.0°
6128	970317	4.00E-6	43.6°	6385	970918	2.29E-7	5.6°
6129	970318		44.6°	6396	970925	2.83E-6	21.9°
6148	970330	4.23E-6	35.0°	6437	971015	4.56E-7	43.4°
6165	970408	3.76E-6	45.0°	6439	971016	9.58E-8	32.1°
6166	970408	7.97E-8	30.3°	6443	971021	1.07E-6	44.9°
6167	970409	9.21E-6	1.4°	6472	971110	2.67E-4	18.1°
6188	970417	3.95E-7	21.4°	6492	971122		43.7°
6209	970426	3.37E-6	28.6°	6523	971207	2.79E-6	43.1°
6213	970429		25.6°	6529	971210	9.00E-7	33.3°
6219	970503	1.47E-7	38.0°	6545	971225	3.56E-6	29.1°
6229	970511		19.7°	6577	980124	1.96E-6	44.7°
6240	970523	2.19E-5	10.7°	6581	980125	4.88E-5	18.2°
6251	970603	4.45E-6	35.1°	6590	980207	1.16E-5	30.1°
6265	970612	7.81E-7	28.7°	6599	980213	4.22E-6	38.1°
6267	970612	1.06E-6	27.6°	6610	980222	4.36E-6	42.8°
6279	970627	7.14E-6	33.9°	6613	980223	5.91E-7	17.1°
6288	970629	2.38E-6	11.5°	6619	980301	6.16E-6	3.7°
6295	970707	6.59E-6	33.5°	6641	980315	5.94E-7	32.4°
6300	970709	4.53E-7	17.9°	6665	980329	8.26E-5	24.1°
6305	970713	7.76E-7	24.0°	6666	980329	1.48E-6	32.9°
6317	970725	8.33E-7	18.2°	6672	980401	7.81E-6	28.2°
6323	970802	2.00E-6	38.0°	6679	980404	2.62E-6	25.7°
6325	970803		28.3°	6694	980420	2.48E-5	34.7°
6338	970817	5.46E-7	24.2°	6702	980424	1.03E-5	44.4°
6358	970903		36.9°	6716	980430	1.53E-6	10.5°
6366	970906	1.86E-5	44.6°	6720	980503	1.49E-6	33.7°

Table 1: The 54 GRBs used in this analysis. Blank spaces indicate that no information was found in the BATSE 4B catalog.

This research was supported in part by the National Science Foundation, the U. S. Department of Energy Office of High Energy Physics, the U. S. Department of Energy Office of Nuclear Physics, Los Alamos National Laboratory, the University of California, the Institute of Geophysics and Planetary Physics, The Research Corporation, and CalSpace.

References

- Briggs, M. et al. 1999, ApJS, preprint, <http://xxx.lanl.gov/abs/astro-ph/9901111>
McCullough, J.F. et al. 1999, these ICRC proceedings
Pilla, R., & Loeb, A. 1998, ApJL, 494, 167
Piran, T. 1999, Phys. Rep., preprint, <http://xxx.lanl.gov/abs/astro-ph/9810256>
Schnee, R. 1996, Ph.D. thesis

Search for Short Duration Bursts of TeV Gamma Rays with the Milagrito Telescope

Gus Sinnis¹ for the Milagro Collaboration

¹ Los Alamos National Laboratory, Los Alamos, NM 87545, USA

Abstract

The Milagrito water Cherenkov telescope operated for over a year (2/97-5/98). The most probable gamma-ray energy was ~ 1 TeV and the trigger rate was as high as 400 Hz. Milagrito has opened a new window on the TeV Universe. We have developed an efficient technique for searching the entire sky for short duration bursts of TeV photons. Such bursts may result from "traditional" gamma-ray bursts that were not in the field-of-view of any other instruments, the evaporation of primordial black holes, or some as yet undiscovered phenomenon. We have begun to search the Milagrito data set for bursts of duration 10 seconds. Here we will present the technique and the expected results. Final results will be presented at the conference.

1 Introduction:

The Milagrito detector is described in detail elsewhere (Westerhoff 1999). The detector operated between February 1997 and May 1998. The event rate varied from 200 Hz to 400 Hz, depending upon the water depth above the photomultiplier tubes (PMTs) and the accumulated rainfall and snowmelt on top of the detector. The energy threshold of Milagrito was below 1 TeV and the most probable energy for gamma rays from zenith was ~ 1 TeV. After a software threshold was applied to the data (we required at least 40 photomultiplier tubes be used in the angle fit), 64% of the data survived and the angular resolution of these events was $\sim 0.7^\circ$ (Wascko 1999). The data set consisted of nearly 6 billion events. Because searching this data set for short duration bursts is computationally intensive; we have developed an algorithm that is relatively efficient. The entire analysis can be run in 10-20 days on a 7-node PC farm.

While there are several reasons to search for short duration bursts (TeV counterparts to gamma-ray bursts, the final stages of black hole evaporation) the most compelling reason may be the discovery potential of a new phenomenon. To our knowledge this is the first such search in this energy regime. In this paper we describe the technique, show results for a subset of the data and calculate the expected sensitivity of the search.

Analysis Technique:

The analysis is a straightforward binned analysis. If one uses square bins, the optimal bin size is 2.8 times the angular resolution of the instrument (Alexandreas, et al., 1993). Given the angular resolution of 0.7 degrees we have used a bin with a 2.0 degree span in declination, and $2.0/\cos(\delta)$ in right ascension. To find the expected background in a given (right ascension/declination) bin we integrate the measured detector efficiency (in local coordinates) over the exposure of that bin. This number is then compared to the actual number of events that fell in the bin. A detailed description of the method follows. For simplicity we have chosen to use hour angle (HA) and declination (δ) as the local coordinate system.

2.0 Background Estimation: The number of events expected in a given time interval from a given direction in the sky is:

$$N_{\text{exp}}(\Delta HA, \Delta \delta) = \iiint \varepsilon[HA(RA, t), \delta] R(t) d(HA) d\delta dt$$

where ε is the efficiency of the detector as a function of the local coordinate system and $R(t)$ is the overall event rate of the detector. The integral is over the angular bin and the time interval in question. The above

equation is only correct if the detector efficiency is constant over the time interval used to estimate the background. The efficiency function $\epsilon(\text{HA}, \delta)$ is obtained from the data in the following manner. Data is collected into maps (2-dimensional arrays) of 0.2×0.2 degree bins (of HA and δ) over two hour intervals. Each map contains the number of events collected in each small bin divided by the total number of events collected over the two-hour interval. This map is therefore a representation of the efficiency of the detector as a function of the local coordinate hour angle and declination. A two-hour interval was chosen to minimize systematic effects caused by any changes in the efficiency function and to obtain sufficient statistics to parameterize the background. To accommodate changes in the detector the integration interval could be shorter than two hours if the detector configuration changed. The background map for each interval was saved to disk.

To perform the integral given above we construct two additional maps of the sky, one for the background and one for the observed sky. Although these maps are in 0.2×0.2 -degree bins, like the efficiency maps, these maps are in "sky" coordinates (right ascension and declination). The observed sky map is constructed by incrementing the appropriate bin for each observed event. The background map is constructed by incrementing every bin by its efficiency (the fraction of events in the contemporaneous 2-hour interval that fell within this bin). Since a simple movement in time relates the right ascension and the hour angle, the updating of the background array is accomplished by rotating the efficiency map to the correct local apparent sidereal time. To improve the performance of the search the background map is updated once every 10 seconds (by $N_{\text{events}} \times \epsilon(\text{HA}, \delta)$). (Note that the sky moves by 0.04 degrees in 10 seconds.)

2.1 Search for an Excess: Since we do not know the start time or the direction of a possible burst we must oversample the sky in both time and space. We use two time bins (each of ten seconds duration), shifted by 5 seconds, and 4 different grids of angular bins. If the first angular grid is centered on (RA, δ) , the remaining grids are centered on $(\text{RA} + 1^\circ / \cos(\delta), \delta)$, $(\text{RA}, \delta + 1^\circ)$, and $(\text{RA} + 1^\circ / \cos(\delta), \delta + 1^\circ)$. Every 5 seconds a 10 second interval completes and all 4 angular grids are searched for an excess. In practice the 4 grids are formed "on-the-fly" by performing the appropriate sums over the 0.2×0.2 degree maps. These sums yield the number of observed events (N_{obs}) and the number of expected events (N_{exp}) in every $2.0 \times 2.0 / \cos(\delta)$ bin. The Poisson probability is calculated and the result is stored in a histogram. If the interval has a Poisson probability less than 10^{-8} the start time, right ascension, declination, N_{exp} , and N_{obs} are also saved.

3 Search Results:

The probability distribution from one day of data is shown in Figure 1. Note that the figure does not contain completely independent entries. The results from each of the 4 angular grids are summed into a single histogram, as are the results from the two offset time bins. The spikes in the distributions are caused by the quantization of the observed and expected number of events. The slope of the distribution is consistent with expectations. No significant burst has been observed in this subset of the data. Figures 2 and 3 show the distribution of the expected number of events and the observed number of events from the same day.

3.1 Flux Upper Limits: If the search completes and no significant burst is found several upper limits may be given. Given the maximum number of observed events over the entire observation period (~1 year), one can derive an absolute upper limit for the entire time period. One can also derive a "typical" upper limit, based on the typical number of events observed in a bin. We report an expected absolute upper limit as a function of zenith angle (since the sensitivity of the detector changes with the zenith angle). This should give an indication of the sensitivity of our search. "Typical" upper limits are roughly 1/4 of the strict upper limit.

3.2 Strict Upper Limit: For the subset of the data searched the maximum number of observed events in any 10-second interval was 15 with a background of 2. Therefore, our 90% confidence level upper limit for the number of source events in any bin is 19.3. Three corrections must be applied to this number before it

can be converted into a flux. First, no more than 48% of any source events should be contained in the signal bin. For a Gaussian response the fraction is 72%, however the angular resolution function of Milagrito has a significant non-Gaussian tail. In addition, in this analysis the sky was binned into 4 overlapping grids, thus there is an efficiency associated with the location of a source falling randomly on the sky. In practice these two effects must be accounted for simultaneously. For the worst case source location the combined correction is 2.4. Finally, two time windows shifted by 5 seconds are used. Thus a 10-second burst starting 2.5 seconds into a window will only have 75% of its events within any time window. Thus, in this scenario if no significant burst were observed the 90% C.L. upper limit on the number of excess events within any 10-second window would be $61.7 = 19.3 \times 2.4 \times 1.3$. To convert this to an upper limit on the flux of gamma rays we must convolute the effective area of Milagrito with an assumed source spectrum, $I_0(E)^{-\alpha}$. If we assume, $\alpha=2$, we may set an upper limit on I_0 . The effective area vs. energy for several ranges of zenith angle is shown in these proceedings (Figure 1 from Westerhoff 1999). The resulting expected upper limits to the flux are tabulated in Table 1.

Zenith Angle Range (degrees)	Median Energy (TeV)	Expected Flux Upper Limit (γ 's $\text{cm}^{-2} \text{sec}^{-1} \text{TeV}^{-1}$) (I_0)
0-15	7.5	7.8×10^{-8}
15-30	9.7	1.29×10^{-7}
30-45	13.2	3.76×10^{-7}

Table 1: Expected 90% C.L. upper limits to the flux of gamma rays for 10-second bursts viewed by Milagrito.

4 Future Work

The software cuts and the size of the angular bin used for this subset of the data has not been optimized for this particular search. Since the expected number of background events is small, the search bin should be larger (Alexandreas 1993). In addition since the source location within the bin is unknown one would expect the optimal bin to be larger yet. Monte Carlo work is in progress to optimize the search technique for this data set, and the response of the Milagrito detector.

5 Conclusions

We have begun to search the Milagrito data set for 10-second bursts from any direction of the sky. So far we have failed to detect any significant bursts of this duration. We have given an indication of the sensitivity of the method by reporting expected flux upper limits in the absence of any detected bursts. Final results will be reported at the conference.

Acknowledgements

This research was supported in part by the National Science Foundation, the U. S. Department of Energy Office of High Energy Physics, the U. S. Department of Energy Office of Nuclear Physics, Los Alamos National Laboratory, the University of California, the California Space Institute, and the Institute of Geophysics and Planetary Physics. We would also like to acknowledge the hard work and dedication of Scott Delay, Michael Schneider, and Neil Thompson, without whom Milagro would still be a dream.

References

Alexandreas, D.E., *et al.* 1993, Nucl. Instr. Meth., **A328**, 570.

Leonor, I. 1999, Proc. 26th ICRC (Salt Lake City, 1999), OG 2.6.06.
Wascko, M. O., 1999, Proc. 26th ICRC (Salt Lake City, 1999), SH 3.2.39.
Westerhoff, S. 1999, Proc. 26th ICRC (Salt Lake City, 1999), OG 2.1.11

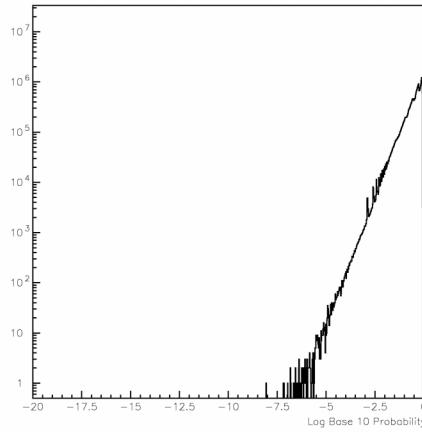


Figure 1: Sample probability distribution from 10-second burst search.

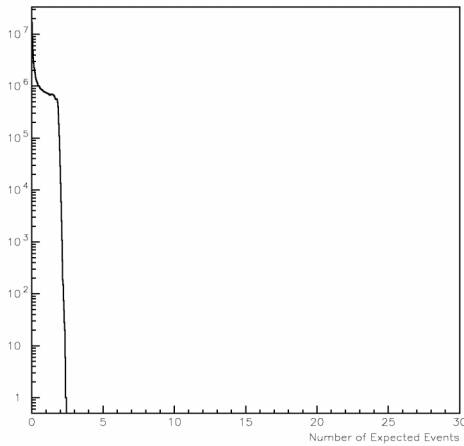


Figure 2: Sample distribution of expected number of events from 10-second burst search.

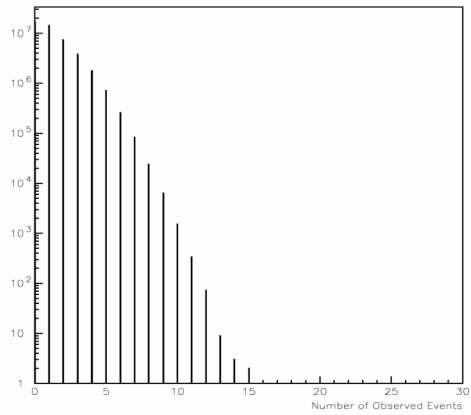


Figure 3: Sample distribution of observed number of events from 10-second burst search.

An All-Sky Search for Steady VHE Gamma-Ray Sources

K. Wang¹ for the Milagro Collaboration

¹Department of Physics, University of California, Riverside, CA 92521, USA

Abstract

The Milagrito water Cherenkov detector in the Jemez Mountains near Los Alamos, New Mexico took data from February 1997 to April 1998. Milagrito served as a prototype for the larger Milagro detector, which has just begun operations. Milagrito was the first large-aperture gamma-ray detector with sensitivity to gamma rays below 1 TeV. We report here on a search for steady emission from point sources over most of the northern sky using data from Milagrito.

1 Introduction:

The discovery of TeV γ -ray sources in the universe has greatly enriched our knowledge of the astrophysics of particle acceleration. TeV (very-high energy, VHE) gamma rays have been observed by air Cherenkov telescopes (ACT) from at least three galactic and three extragalactic sources (see, for example, Ong, 1998; Hoffman et al., 1999). In addition, ACTs have searched for VHE emission from a number of other sources including some supernova remnants and other blazars. These searches have generally involved exposures of only a few hours to a particular source so they may have missed highly variable sources such as blazars. Because an ACT is a pointed instrument with a field of view of only several millisteradians, there has been no all-sky search for VHE sources. There have been several all-sky searches at higher energies using scintillator arrays with negative results (Alexandreas et al., 1991; McKay et al., 1993).

Milagrito was built and operated as a prototype for the Milagro detector (McCullough *et al.*, 1999). Milagrito, which took data from February 1997 to April 1998, had 228 photomultiplier tubes (PMTs) on a $3 \times 3 \text{ m}^2$ grid under 0.9 m of water. The properties of Milagrito are discussed elsewhere in these Proceedings (Westerhoff *et al.*, 1999). Nearly 9×10^9 events were recorded from Milagrito. Milagrito was the first air-shower array with sensitivity to gamma rays below 1 TeV. Because Milagrito had a large field of view ($>1 \text{ sr}$) and operated all the time, it can be used to search for steady VHE sources anywhere in the northern sky. The sky coverage of Milagrito is illustrated in Figure 1.

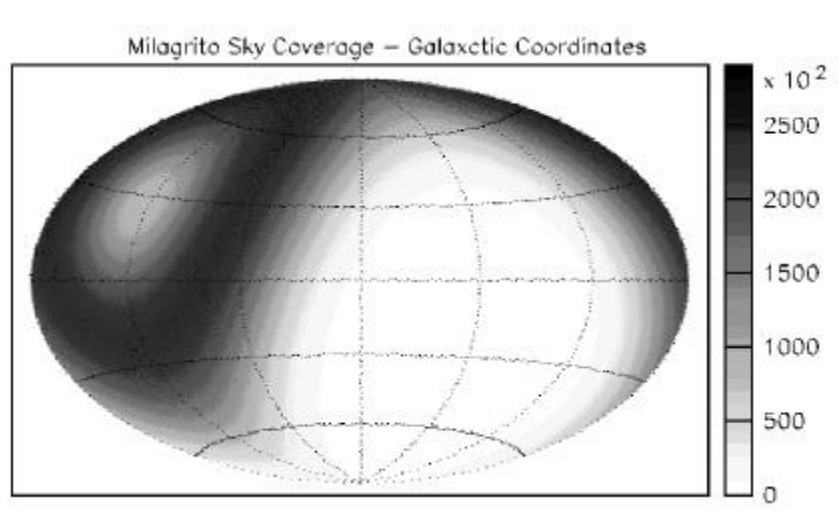


Figure 1. The density of events from Milagrito (in arbitrary units) plotted in galactic coordinates.

2 Technique:

The all-sky search for steady TeV sources is performed by dividing the sky into a grid of non-overlapping bins in celestial coordinates, right ascension (RA) and declination (δ). To search for VHE emission from point sources, the number of events in each bin for the entire data set is tabulated and compared with the expected number of background events from cosmic rays. A description of the background estimation method has been discussed in Alexandreas (1993). Because a point source could lie near the edge of a bin, additional searches are made with grids offset in RA, in δ , and in both RA and δ . The bin size is chosen to maximize the significance of a signal in that bin. For a Gaussian angular resolution, this bin is $\pm 1.4\sigma$ in declination and $\pm 1.4\sigma/\cos(\delta)$ in right ascension, where σ is the rms angular resolution.

The shower direction is calculated from the relative times at which the PMTs are struck after correcting for the effects of electronic slewing, sampling of particles in the shower front, and curvature of the shower front. After making these corrections, the direction of the shower plane can be determined with a least squares fit using the measured times and positions from the PMTs; in reality, some modifications to a straightforward least squares fit are needed to account for the tail of late light due to low-energy particles that tend to trail the shower front and nearly horizontal light in the water from the large Cerenkov angle and from scattering of particles and light in the water. Baffles have been installed around the PMTs in Milagro to block the horizontal light.

Detailed studies of the Milagro angular resolution have been performed using both data and Monte Carlo simulations. The uncertainty in the reconstructed shower direction can be studied with data using DELEO, which is obtained by fitting each shower with two independent, interleaved portions of the detector (the detector is divided as light and dark squares of a checkerboard) and computing the difference in the fit space angles. DELEO is not sensitive to certain systematic errors such as those due to core location errors. In the absence of these systematic effects, DELEO should be about twice the overall angular resolution (Alexandreas *et al.*, 1992). Figure 2 shows the median DELEO for Milagro data as a function of the minimum number of PMTs in the fit (NFIT). This shows that the angular resolution is a strong function of NFIT.

The angular resolution can also be obtained from a study of the observed shadow of the moon, after correcting for the bending of the cosmic rays in the earth's magnetic field (Wascko *et al.*, 1999). Unlike DELEO, this technique can reveal systematic pointing errors.

Both of these techniques only address the angular resolution for hadron-induced showers. Monte Carlo simulations are used to compare the expected DELEO distribution for cosmic ray showers to the measured DELEO distribution, and to compare the overall angular resolution for cosmic-ray and photon-induced events. Based on this information, a bin size of $\pm 1.1^\circ$ in declination and $\pm(1.1/\cos(\delta))^\circ$ in right ascension has been chosen for the all-sky search.

In addition, an unbinned search for sources has been performed based on the wavelet formalism. The spatial scale size of this analysis can be varied allowing both point and extended sources to be identified.

Results of the search for steady VHE emission from point sources from these data will be presented, and the sensitivities of the two search techniques will be given. These searches would detect a point source at $\delta = 36^\circ$ (*i. e.* passing overhead) with a steady flux above 1 TeV larger than about $10^{-6} \text{ m}^{-2} \text{ s}^{-1}$, assuming a spectral shape similar to that of the Crab. The sensitivity decreases for sources at other declinations; the flux required for detection of a source at $\delta = 25^\circ$ is about 15% larger.

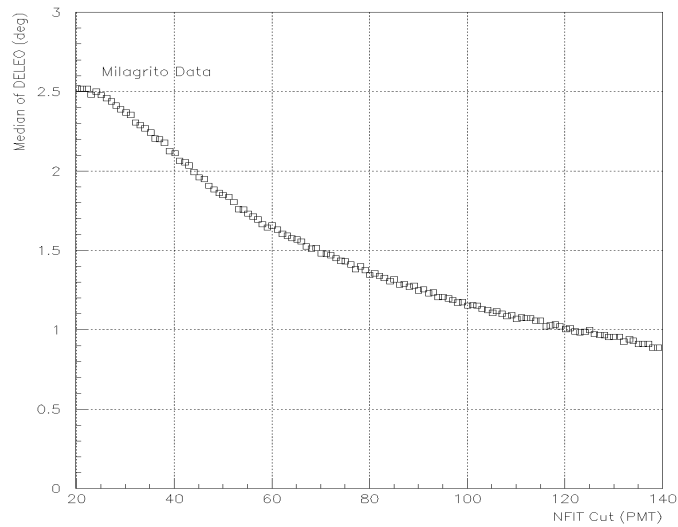


Figure 2. The median DELEO vs. the minimum number of PMTs used in the fit (NFIT) for Milagrito data.

This work was supported in part by the National Science Foundation, The U. S. Department of Energy Office of High Energy Physics, The U. S. Department of Energy Office of Nuclear Physics, Los Alamos National Laboratory, the University of California, the Institute of Geophysics and Planetary Physics, The Research Corporation, and the California Space Institute.

References

- Alexandreas, D. E. *et al.*, ApJ, **383**, L53 (1991).
 Alexandreas, D. E. *et al.*, Nucl. Instr. Meth., **A311**, 350 (1992).
 Alexandreas, D. E. *et al.*, Nucl. Instr. Meth., **A328**, 570 (1993).
 Hoffman, C. M., C. Sinnis, P. Fleury, and M. Punch, to be published in Rev. Mod. Phys. (1999).
 McCullough, J. F. *et al.*, 1999, these Proceedings, paper HE 6.1.02.
 McKay, T. A. *et al.*, Ap. J. **417**, 742 (1993).
 Ong, R. A., Phys. Rep., **305**, 93 (1998).
 Wascko, M. *et al.*, 1999, these Proceedings, paper SH.3.2.39
 Westerhoff, S. *et al.*, 1999, these Proceedings, paper OG 2.1.11.

Atmospheric Cherenkov Detectors at Milagro to Measure Cosmic-Ray Composition Above 50 TeV

R. Atkins¹, B. Bravar², B.L. Dingus¹, D. Evans³, J.A. Goodman³, T.J. Haines⁴, T. Harrison⁵, C.M. Hoffman⁴, L.A. Kelley⁶, A.J. Matthews⁷, J. McCullough⁶, J.E. McEnery¹, P. Nemethy⁸, G. Sennis⁴, T.E. Stephens⁵, S.J. Stochaj⁹, O.T. Tumer¹⁰, M. Wascko¹¹, D.A. Williams⁶, and G.B. Yodh¹²

¹*Department of Physics, University of Utah, Salt Lake City, UT 84112, USA*

²*Particle Astrophysics Lab, New Mexico State University, Las Cruces, NM 88003, USA*

³*Department of Physics, University of Maryland, College Park, MD 20742, USA*

⁴*Los Alamos National Laboratory, Los Alamos, NM 87545, USA*

⁵*Department of Astronomy, New Mexico State University, Las Cruces, NM 88003, USA*

⁶*Santa Cruz Institute for Particle Physics, University of California, Santa Cruz, CA 95064, USA*

⁷*New Mexico Center for Particle Physics, University of New Mexico, Albuquerque, NM 87131, USA*

⁸*Department of Physics, New York University, New York NY 10003, USA*

⁹*Department of Elec. and Comp. Engineering, New Mexico State University, Las Cruces, NM 88003, USA*

¹⁰*Institute of Geophysics and Planetary Physics, University of California, Riverside, CA 92521, USA*

¹¹*Department of Physics, University of California, Riverside, CA 92521, USA*

¹²*Department of Physics and Astronomy, University of California Irvine, Irvine, CA 92697, USA*

Abstract

The Wide Angle Cherenkov Telescope (WACT) experiment is currently being constructed at the Fenton Hill Observatory, located near Los Alamos, New Mexico. WACT consists of six air Cherenkov telescopes, each with 3.8 m² mirrors, distributed over an area of about 60,000 square meters. WACT samples the lateral distribution of Cherenkov light from cosmic rays at various distances from the core and is thus sensitive to the height of maximum shower development. WACT is being built around the Milagro gamma-ray observatory. Milagro has the ability to locate the core and measure the hadronic and muon content of the extensive air showers. These features are crucial to the determination of the cosmic-ray composition. WACT will be the first ground based detector capable of determining the cosmic-ray composition from above 10¹⁶ eV down to energies where it has been directly measured by balloon-borne instruments. A general overview, construction status, and preliminary simulation results will be presented.

1 Introduction:

Nearly a century after the discovery of cosmic-rays there is still a great deal we do not know about them. Detection of cosmic-rays is usually accomplished in one of two ways. Cosmic rays are directly measured with balloon and space borne emulsion detectors, or other types of particle detectors high in the atmosphere. This technique is limited by the size of the detector and is not well suited for measuring cosmic-ray fluxes at energies above 10¹⁵ eV. The second technique uses extensive air showers (EAS) in which the primary creates a cascade of secondary particles that can be detected. These secondary particles can be observed by the Cherenkov radiation they emit, by direct detection of the particles in scintillator arrays, with underground detectors, or by nitrogen fluorescence in the atmosphere. These methods can have large effective areas, but are complicated in that one does not directly observe the primary particle (Cronin, 1999).

The observed energy spectrum of cosmic rays is a power law that falls like $E^{-2.7}$ (Gaisser, 1990). Above 10¹⁶ eV the spectrum steepens to $E^{-3.0}$. This change in spectral index, known as the knee, occurs between 10¹⁵ eV and 10¹⁶ eV and has been of great interest. If the knee represents a change from Galactic to extragalactic cosmic-rays, then one would expect an increasingly lighter composition at higher energies. This could be due to a change in predominant accelerations mechanisms or photo-disassociation of heavier nuclei in the sources. If the knee is a result of increased leakage from the Galaxy, then one would expect to see a heavier

composition above the knee. This is due to magnetic confinement effects in the Galaxy. The ability of the Galaxy to confine a particle is a function of that particles rigidity, pc/Z . Thus, the larger the rigidity the less likely a particle is to be confined in the Galaxy. Unfortunately the knee occurs in an energy regime where the preferred experimental technique also changes and is therefore difficult to measure. The primary objective of WACT is to measure the cosmic ray composition in this region.

Most of the information that we currently have on composition below the knee has been obtained by balloon and space based experiments. Balloon and space experiments can determine the cosmic-ray composition on an event-by-event basis. However they have small effective areas and thus cannot make measurements above the knee due to the smaller flux. Measurement of cosmic-ray composition above the knee has been done with the EAS technique.

There are many different type of EAS techniques, but the primary goal is to observe the particles in the shower. Recent experiments using EAS techniques have shown that the knee is not as sharp, as was previously believed (Amenomori et al., 1996). There are, however, some discrepancies in the results of different EAS experiments in regards to composition. For instance DICE (dual imaging Cherenkov experiment) reported a trend towards lighter nuclei above the knee (Boothby et al., 1997), while other experiments have reported a more massive composition (Bernlöhner et al., 1998). Better measurements of composition in this energy regime are necessary to achieve an understanding of the physical processes governing the acceleration of cosmic-rays. Figure 1 shows different shower max measurements from various experiments. Shower max is a measurement of the depth at which one finds the largest number of particles in an EAS. This depth is sensitive to composition.

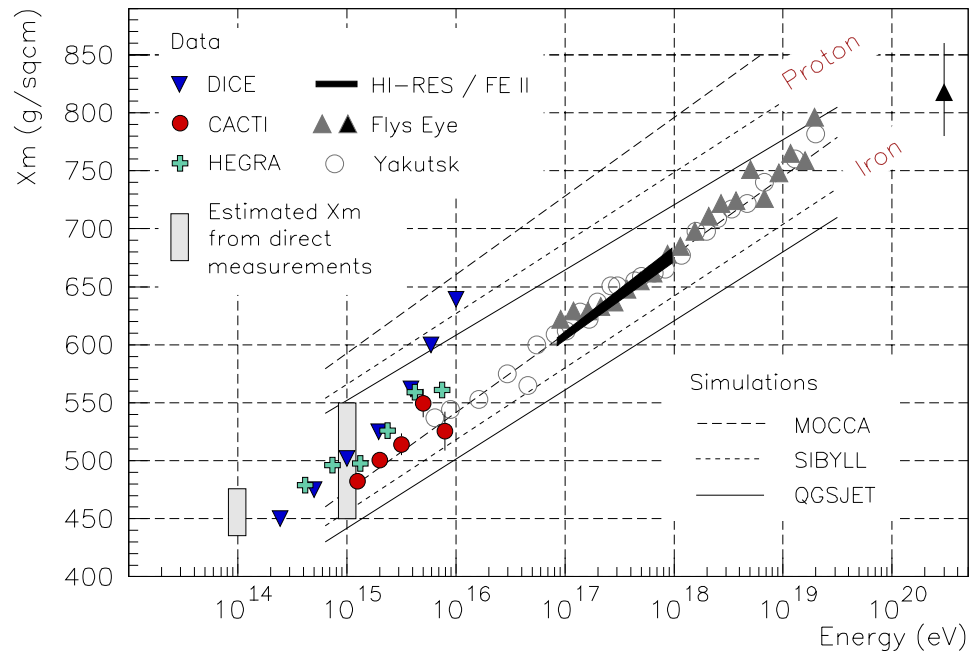


Figure 1: Measured and inferred shower max from different experiments. The solid and dashed lines represent expected shower max from different simulations. Note the trend towards lighter nuclei reported by DICE. It should also be noted that the last to DICE points have large error bars that are not shown (Paling, 1997).

2 Experimental Technique and Description

The technique that WACT will use to determine cosmic-ray composition is based on the sensitivity of the lateral distribution of Cherenkov light to the depth of shower max (Patterson & Hillas, 1983). Most of the Cherenkov light generated in an EAS is created at shower max. One would expect to see a flatter lateral distribution for showers initiated by particles that interact higher in the atmosphere. Therefore, a measurement of the Cherenkov distribution will yield the depth of shower max. The number of Cherenkov photons in an EAS depends on the energy of the primary particle.

To determine the energy of the primary particle and the species WACT will make measurements of the Cherenkov light at various distance from the core. The intensity of the Cherenkov light far from the shower core determines the energy of the primary. CORSIKA simulations have shown that the logarithm of lateral distribution of Cherenkov light varies with the distance to shower core but is close to linear over the region from 50 to 200 meters. The slope of the fitted line depends on composition as seen in Figure 2, and the intercept at 140 meters is a good indicator of primary energy.

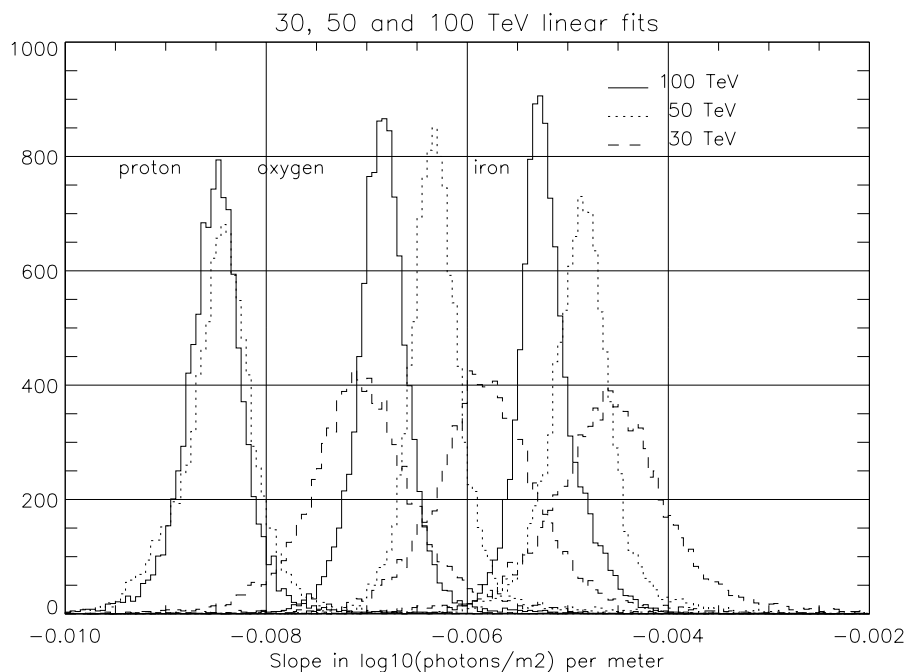


Figure 2: Measured slopes from CORSIKA simulations for different energy and different species. These slopes are measured in the linear region of the lateral distribution of Cherenkov radiation.

WACT will consist of six Cherenkov telescopes surrounding the Milagro gamma-ray observatory; 3 telescopes at about 60 m from the center of the pond and 3 telescope at 120 meters from the pond. Each telescope has a 3.8 m² spherical mirror of focal length 2.35 meters. Suspended over the mirror will be a camera consisting of 20 to 25 two-inch diameter PMT's each with a light cone to give a field of view of 2 degrees per PMT. Each telescope is placed on a cement pad and is covered by a steel frame cloth building that can slide off the pad during periods of operation. WACT will have an effective area of about 60,000 m² for showers with 2 telescopes close to the shower core (30 meters) and two or more located around 100 meters from the core.

Milagro is a gamma ray observatory that detects the Cherenkov light generated in water by the secondary particles of the EAS. It consists of a covered pond that has a geometric area of about 5000 square meters located at 2650m above sea level (750g/cm²). Two layers of PMT's are suspended in the water. The top layer of tubes is below 1.5 meters of water and the bottom layer (hadron layer) is below 6.5 meters of water. Unlike other ground arrays, Milagro has a fully sensitive area, thus it can directly observe nearly all the particles (in the 5000 m² area) in an EAS at ground level. The combination of Milagro and WACT will allow a measurement of the atmospheric Cherenkov light from the shower, the core location, the electron, muon, and hadronic content of the shower, and the energy and direction of the primary. It is this combination that allows us to make a complete picture of the EAS. The WACT data will be bundled with the Milagro data stream and will use the same time over threshold (TOT) method used in Milagro to measure the PMT signal size. The TOT method works, as the name implies, by measuring the time that the signal from a given tube is above a predetermined threshold. This time is approximately proportional to the logarithm of the pulse charge (Atkins et al.). By using the TOT method we can use the electronics already developed by the Milagro experiment with minor modifications. This not only simplifies the development of the electronics, but is also less expensive in that the TOT method does not require the use of analog to digital converters.

3 Status and Future

The WACT experiment is in the early stages of construction. The mirrors are the prototypes from the Hi-Res Fly's Eye cosmic-ray experiment and have been prepared for use with WACT. Construction of the building for the first telescope will be completed by the end of April 1999. PMT testing is being done at Los Alamos National Lab and electronics are being provided by the University of California at Santa Cruz. The night sky background has been measured and is low enough to use the TOT method. By the end of the summer of 1999 we should have completed a prototype telescope at Fenton Hill. By the summer of 2000 we should have completed all six telescopes and will start full data taking. A full detector simulation is currently being prepared at Los Alamos and at New Mexico State.

4 Conclusions

The WACT experiment will provide information about cosmic-ray composition above and below the knee, and will therefore be able to overlap with both direct and indirect measurements. The combination of WACT and Milagro will provide a more complete picture of extensive air-showers in this energy range above and below the knee. WACT will also provide a way of checking the energy resolution and angular resolution of Milagro.

5 Acknowledgements

The WACT collaboration would like to thank the Hi-Res Fly's Eye experiment for mirrors for WACT. We would also like to thank Milagro collaboration, Scott Delay, David Kieda, Stan Thomas, Joe Herrera, and Gary McDonough for their technical support and assistance. This work is supported in part by the National Science Foundation, the U.S. Department of Energy Offices of High Energy Physics and Nuclear Physics, the University of California, Los Alamos National Laboratory, the U.C. Institute of Geophysics and Planetary Physics, and Research Corporation.

□ Atmospheric Cerenkov Telescope (ACT) with 3.8 m² mirror

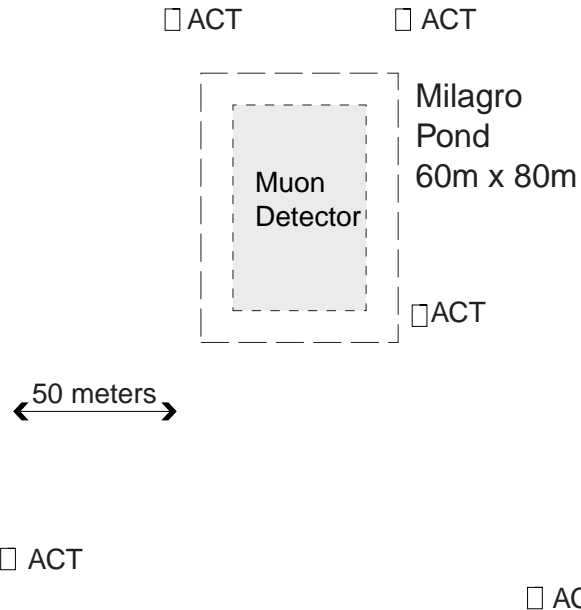


Figure 3: Placement of WACT telescopes relative to Milagro.

References

- Amenomori, M. et al. 1996, ApJ 461, 408
- Atkins, R. et al. 1999, Proceedings from the 26th ICRC
- Berndlöhr, K. et al. 1998, Astrop. Phys. 8 253
- Boothby K. et al. 1997, ApJL 491, L35
- Cronin, J.W. 1999, Rev. Mod. Phys. 71 2 S165
- Gaisser, T.K. 1990, Cosmic Rays and Particle Physics (New York: Cambridge University Press)
- Paling, S.M. 1997, Ph.D. Thesis, Dept. of Physics and Astronomy, University of Leeds
- Patterson, J.R. & Hillas, A.M. 1983, J. PHYS. G: Nucl. Phys. 9 1433

Calibration of the Milagro Cosmic Ray telescope.

Lazar Fleysher¹ for the Milagro Collaboration

¹*Department of Physics, New York University, New York, NY 10003, USA*

Abstract

The Milagro detector is an air shower array which uses the water Cherenkov technique and is capable of continuously monitoring the sky at energies near 1 TeV. The detector consists of 20000 metric tons of pure water instrumented with 723 photo-multiplier tubes (PMTs). The PMTs are arranged in a two-layer structure on a lattice of 3 m spacing covering 5000 m^2 area. The direction of the shower is determined from the relative timing of the PMT signals, necessitating a common time reference and amplitude slewing corrections to improve the time resolution. The calibration system to provide these consists of a pulsed laser driving 30 diffusing light sources deployed in the pond to allow cross-calibration of the PMTs. The system is capable of calibrating times and the pulse-heights from the PMTs using the time-over-threshold technique. The absolute energy scale is provided using single muons passing through the detector. The description of the calibration system of the Milagro detector and its prototype Milagrino will be presented.

1 Introduction

This paper describes the method which was used to calibrate the prototype called Milagrino and the Milagro detectors. Milagrino physics results are reported elsewhere in these proceedings. The layout of Milagro detector is described in (McCullough et al., 1999), but, for clarity, some information is provided here.

Milagro is the first detector designed to study air showers at energies near 1 TeV using water Cherenkov techniques. The detector is built in the Jemez Mountains near Los Alamos, New Mexico at an altitude of 2650 m. The pond, which is 60m x 80m x 8m, is filled with clean water, covered with a light barrier and instrumented with 723 - 20 cm PMT's.

The PMTs collect Cherenkov light produced by the shower particles which traverse the detector's water volume. Whenever a PMT pulse exceeds a preset discriminator threshold a multihit time-to-digital converter (TDC) is started. Each PMT has its own TDC which is capable of recording up to 16 discriminator level crossings per event with 0.5 ns resolution. These constitute the raw data from the PMT.

The calibration procedure described below is applied in order to transform the raw counts to physically meaningful arrival times and light intensities which then can be used for event reconstruction. Considerable effort has been made to construct all PMT channels of the detector as uniformly as possible. However to achieve the high precision required for the event reconstruction, the remaining variations between channels have to be compensated for. A separate set of calibration parameters is determined for each PMT channel.

The calibration system has been designed to reflect the physics goals of the detector and is capable of calibrating the times recorded by each PMT to provide the best available shower direction; it is capable of calibrating the "pulse-heights" from the PMTs needed to estimate the absolute energy of each event. The absolute time of the events is retrieved from the GPS (Global Positioning System) clock system to 100 ns accuracy.

1.1 Pointing The desire to reconstruct the position of events on the Celestial sphere with systematic errors $\ll 1^\circ$ dictates that the locations of the photo-tubes be known to about 10 cm accuracy in horizontal direction and about 3 cm in vertical. To meet this requirement, photographic and theodolite surveys of the pond have been performed. At the end of the construction period, when the pond was filled with water, an "as-built" measurement of the elevation of all PMTs has been made.

Knowledge of the PMT coordinates is necessary, although not sufficient, to achieve the stated goal. Times, registered by PMTs, have to have resolution of about 1 ns. This is limited by the transit time jitter of the PMTs at low light levels. Thus, it is important to calibrate the TDC conversion factors, compensate for the

PMT-pulse amplitude dependence of TDC measurements (known as a slewing correction) and synchronize all TDCs (find TDC time offsets) to the required accuracy.

1.2 Energy The relative “pulse-height”-to-photo-electron conversion must be determined to convert all amplitude measurements to a common unit for each event. The photo-electron counts (PEs) then has to be converted to the absolute scale of the energy deposited in the water to reconstruct the shower size and, ultimately, to estimate the energy of the primary particle.

2 Time-over-Threshold

Traditionally, the area of the PMT pulses is measured using amplitude-to-digital converters (ADCs). The major draw-back of this method is that ADCs have narrow dynamic range and are relatively slow devices which causes dead time during data taking. A new technique has been developed to overcome these problems.

The idea behind the Time-over-Threshold (ToT) method is simple. The PMT pulse quickly charges a capacitor C , which is then slowly discharged via a load resistor R . In such a setup the total area of a PMT pulse can be measured by the discharge time (time over threshold).

This method will work only if the time between registered pulses is greater than the discharge time constant $\tau = RC$. Two small pulses not separated in time will appear as one large pulse. To avoid this problem and for noise reduction, a second higher threshold level had been introduced. Now true large pulses cross both thresholds and time-over-high-threshold (HiToT) is a much better measure of the pulse area. It also provides a method of separating small single pulses from everything else.

Similarly, the PMT pulse amplitude is related to ToT and the pulse amplitude dependence of TDC measurements can be compensated using ToT.

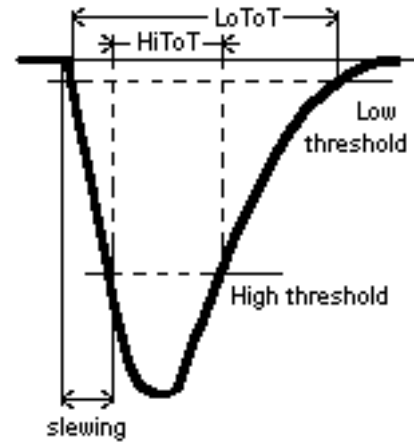


Figure 1: Time-over-Threshold concept.

3 Laser calibration system: description

The Milagro calibration system is based on the laser – fiber-optic – diffusing ball concept used in other water-Cherenkov detectors (See, for instance, Becker-Szendy et al., 1995). A computer operated motion controller drives a neutral density filter wheel to attenuate a pulsed nitrogen dye laser beam. The beam is directed to one of the thirty diffusing laser balls through the fiber-optic switch (See Fig 2). Part of the laser beam is sent to a photo-diode. When triggered by the photo-diode, the pulse-delay generator sends a trigger pulse to the data acquisition system. The balls are floating in the pond so that each PMT can “see” more than one light source. Such a redundant setup allows us to calibrate the PMTs and the electronics.

4 Timing calibration

Because of finite rise-time of a PMT pulse, its registration time depends on the amplitude of the signal. The corrections were found by studying how TDC outputs vary as a function of PMT-pulse ToT. For different laser pulse intensities, the time of registration (t_{reg}) of the PMT response by its TDC with respect to the photo-diode “zero” and ToT were measured. The slewing correcting curve was found by fitting a polynomial to t_{reg} vs ToT .

However, since all the time measurements are done with respect to the photo-diode, the slewing curve is artificially shifted by fiber-optic delay, light travel time in water and TDC time offsets. Knowing the locations of the diffusing laser balls and PMTs, the speed of light in water and fiber-optic delay, the TDC offsets can be found.

This procedure has been repeated for both low and high thresholds (LoToT and HiToT) for each PMT-TDC channel. Now, a meaningful interpretation for the TDC outputs exists.

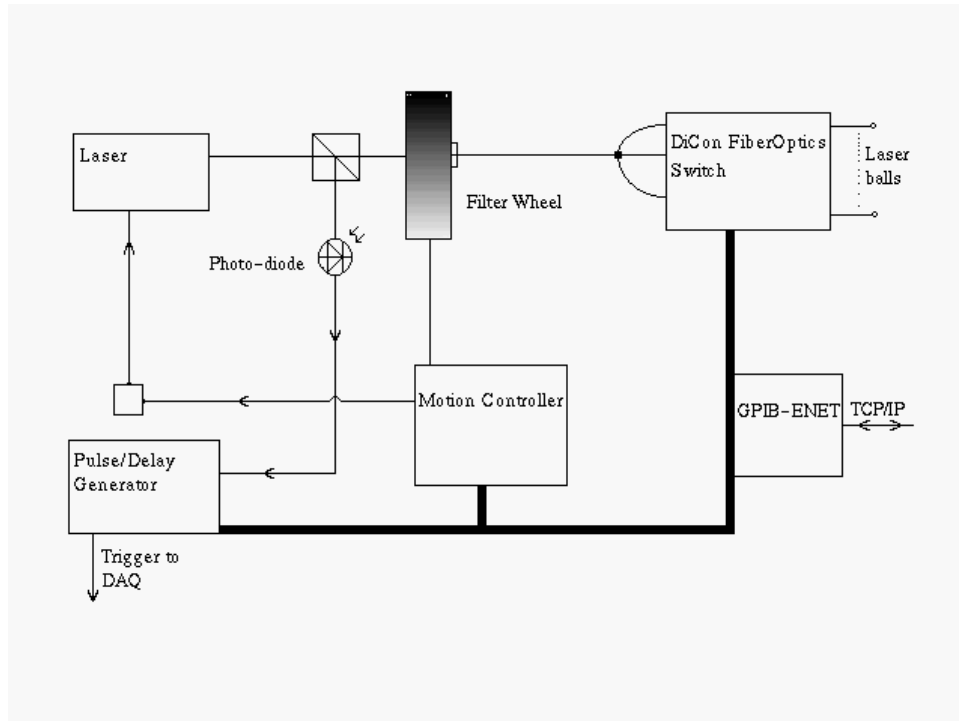


Figure 2: Calibration system setup

5 Consistency check

The Milagro calibration system has been designed to allow cross-calibration of the PMTs. This fact was used to check the accuracy of the obtained calibration parameters and disclose some problems.

TDC time offsets obtained for a given PMT from different laser balls should be identical. Thus, the TDC-offset mismatch distribution becomes a useful diagnostic tool. The mean mismatch in offsets over all PMTs from two laser balls gives the fiber-optic delay difference between them. The width of the mismatch distribution is a measure of the offset quality. In fact, if we used a wrong speed of light in water, it would widen the mismatch distribution. Eventually, this allowed us to determine the effective speed of light in the pond water to four decimal places, by comparing measured offsets from a pair of far separated laser balls.

Another use of redundancy was the reconstruction of laser ball coordinates. Direct reconstruction of the coordinates by reversing the procedure in section 4 will yield either a perfect result or will lead to an inconsistency. In either case, it will not give any constructive information. To overcome this difficulty, a method of pairwise correlations was developed to obtain the laser ball locations. The positions of two laser balls s_1 and s_2 can be obtained by comparing relative time differences from the pair as observed by a PMT. If we define:

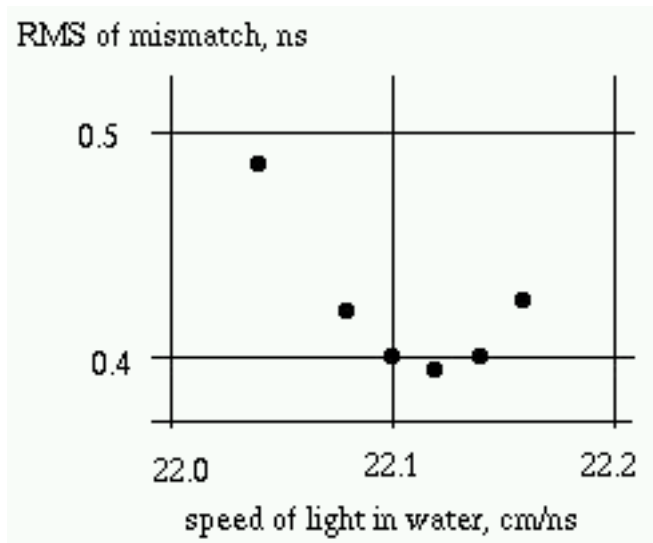


Figure 3: Width of the TDC-offset mismatch distribution as a function of speed of light in water.

$$\tau = t_{s1 \rightarrow PMT} - t_{s2 \rightarrow PMT}$$

where $t_{s1 \rightarrow PMT}$ and $t_{s2 \rightarrow PMT}$ are TDC times, then τ does not depend on the TDC time offset for the particular PMT channel. From geometrical point of view, a given PMT lies on a branch of hyperbola, defined by parameter τ and with the laser balls $s1$ and $s2$ at its foci. Thus, four different PMTs with their corresponding τ 's for the same laser ball pair would define the coordinates of the foci; by using more PMTs the problem becomes overconstrained and yields a best fit. This procedure was used successfully to reconstruct laser ball coordinates for Milagrito and Milagro.

6 Energy calibration

The ToT information was converted to a pulse amplitude scale by moving a set of ADCs to all PMT channels and collecting simultaneous ToT and ADC data. The single photo-electron peak was clearly visible yielding the ToT-to-PE conversion, assuming the ADC outputs are linear in the number of PEs. Alternatively, assuming that the number of registered PEs obeys a Poisson distribution, the occupancy method was used to obtain the ToT-to-PE calibration. Both methods are in reasonable agreement.

Absolute energy calibration measurements will be done using through-going muons. The imaging capabilities of the detector will be exploited in order to find, fit and select well-defined through-going muon tracks. Once the geometry of the track is known, the Cherenkov energy deposit will be estimated and compared against the photo-electron distribution in the event. This was the primary absolute energy calibration method used in the IMB detector (Becker-Szendy et al., 1995).

7 Acknowledgment

This research was supported in part by the National Science Foundation, the U. S. Department of Energy Office of High Energy Physics, the U. S. Department of Energy Office of Nuclear Physics, Los Alamos National Laboratory, the University of California, the Institute of Geophysics and Planetary Physics, The Research Corporation, and the California Space Institute.

References

- Becker-Szendy, R. et al., Nucl. Instr. and Meth. A **352** 629 (1995)
McCullough, J. et al., Proc. 26th ICRC (Salt Lake City, 1999), HE.6.1.02

Use of Instrumented Water Tanks for the Improvement of Air Shower Detector Sensitivity

Anthony L. Shoup¹, for the Milagro Collaboration

¹*Department of Physics and Astronomy, University of California, Irvine, CA, 92697*

Abstract

Previous works have shown that water Cherenkov detectors have superior sensitivity to those of scintillation counters as applied to detecting extensive air showers (EAS). This is in large part due to their much higher sensitivity to EAS photons which are more than five times more numerous than EAS electrons. Large area water Cherenkov detectors can be constructed relatively cheaply and operated reliably. A sparse detector array has been designed which uses these types of detectors to substantially increase the area over which the Milagro Gamma Ray Observatory collects EAS information. Improvements to the Milagro detector's performance characteristics and sensitivity derived from this array and preliminary results from a prototype array currently installed near the Milagro detector will be presented.

1 Introduction

The field of Very High Energy (VHE) gamma-ray astronomy has exploded in recent years, mainly pushed by the development of more sensitive telescopes. The emphasis has been to lower energy thresholds, improve angular and energy resolutions and most importantly hadronic cosmic ray background rejection.

Considerable efforts have also been made to develop telescopes which detect VHE extensive air showers (EAS) which have secondaries that survive to ground level, such as Milagro and the Tibet Array. If reasonable sensitivity at VHE energies can be achieved with these detectors, they will offer powerful capabilities, such as full overhead sky coverage both day and night regardless of weather and skylight conditions. This would allow much higher temporal coverage of sources that are already known to be highly variable, such as Active Galactic Nuclei.

The Milagro detector is progressing toward reaching the necessary VHE sensitivity. It is a large (60m x 80m x 8m) water pond instrumented with 723 8" photomultiplier tubes (pmts) in two layers. These pmts detect the Cherenkov light produced by EAS secondaries passing through the optically clear water. Its high altitude (2650m) and sensitivity to both photonic and leptonic EAS components give it an energy threshold such that for zenith traversing sources the peak primary energy will be 1 TeV. After calibrations it will have good angular resolution and hadronic cosmic ray rejection (see McCullough 1999 for more details).

To improve the sensitivity of the current Milagro detector, 172 instrumented, large area (5m²), water Cherenkov detectors (tanks) will be deployed around the pond to effectively extend its active area. As discussed below, this will improve both the energy and angular resolution of Milagro and increase its hadronic cosmic ray rejection, thus improving its overall VHE sensitivity. It can also be used to increase Milagro's efficiency for detecting EAS below 1.0 TeV which have core positions significantly away from the Milagro pond.

2 Water Tank Detector & Array

The criteria for selecting a detector design that will improve the performance of EAS experiments are: low cost and low maintenance (a large ground area needs to be covered, typically at a remote high altitude site), high sensitivity to EAS secondary particles, and good timing and particle density resolution. Previous works (Yodh 1996) showed that water Cherenkov detectors have superior sensitivity to those of scintillation counters for detecting EAS secondaries. Thus the tank design proposed here satisfies these design criteria, although the particle density resolution is somewhat poor. On average the pmt signal is about 100 photoelectrons for a through-going vertical muon.

Figure 1 displays a cross-sectional view of a tank showing the position of the top-mounted, downward-looking 8" pmt and the Tyvek-lined bottom, sides, and floating top. This position of the pmt gives a fairly uniform response across the full tank, although it does degrade the timing resolution somewhat compared to a bottom mounted, upward looking position. Due to its active material, water, the tank is sensitive to both the photonic and leptonic components of EAS as opposed to plastic scintillator based detectors which are mainly sensitive to the leptonic component. The Tyvek lining provides a diffusively reflective inner surface with $> 90\%$ reflectivity at the important wavelengths determined from convoluting the Cherenkov photon spectrum and pmt quantum efficiency (wavelengths around 350 nm).

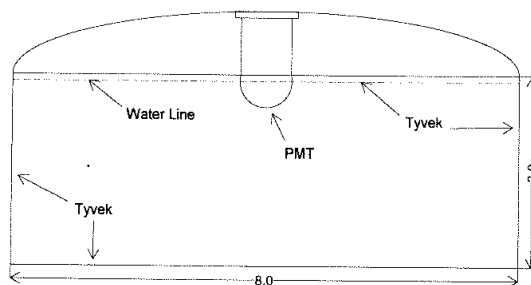


Figure 1: Schematic of example water Cherenkov tank. Key features are top mounted, downward looking pmt and Tyvek lined inner surfaces (units are feet).

The Milagro inspired tank array has 172 tanks placed on a square grid with a spacing of 15 m, giving a full array area of 200m x 200m centered on the Milagro pond.

Monte Carlo generated data was used to determine the performance characteristics of these tanks, and the improvement of the sensitivity of the Milagro detector generated by using these tanks. Corsika was used for generating simulated EAS and the Geant package was used to simulate the tank and Milagro detector responses (see (Westerhoff 1998) for more details).

3 Monte Carlo Estimates of Milagro Performance Improvements

The information acquired with the tanks discussed above can be used in two separate ways. First, it may improve the angular and energy reconstruction resolutions of EAS which trigger the Milagro pond detector by making additional independent shower front timing measurements and by improving the EAS core position resolution for EAS whose cores do not strike the pond. A simple multiplicity trigger condition of 50 pond pmts being hit by an EAS was used as a pond-trigger in simulations. Second, the information can be used to increase the effective area of the Milagro detector by using it in a combined pond-tank trigger.

3.1 Improvements in Pond Triggered Events From simulation, on average about 24 tank pmts are hit per event where a hit is the detection of 1 or more photoelectrons. The occupancy (fraction of the time a given pmt or tank is hit) for pond pmts is about 30% and for tanks is about 10%. The tanks have fewer low pulse height hits than the pond pmts (below 30 pes) but about the same number of large pulseheight hits (above 30 pes).

As seen in Figure 2, our simulations predict that using the tank array in reconstructing EAS core positions can improve the position resolution tremendously for EAS whose core positions are off the pond. This improvement is crucial for EAS energy determination and is also important in EAS angle determination because the pmt hit times must be corrected for EAS shower front curvature about the core position. Current ongoing studies of Monte Carlo generated EAS show that a good core position resolution should improve the hadronic cosmic ray rejection capabilities of Milagro as well.

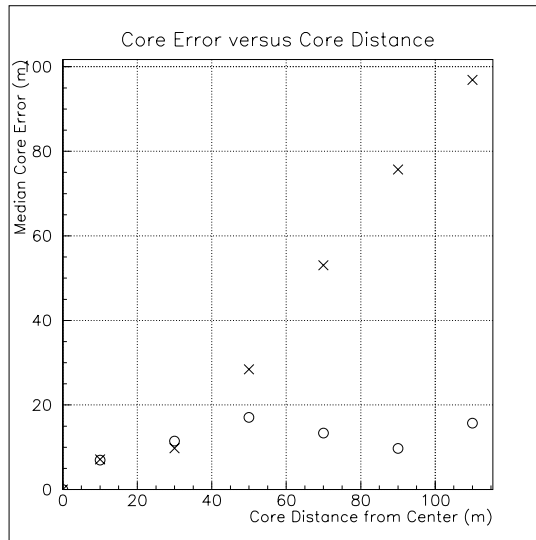


Figure 2: Plot of median core position error versus core distance from center of Milagro pond using tanks (circles) and not using tanks (crosses).

Improvements in the angular reconstruction resolution of EAS is displayed in Figure 3. The improvement is maximal for low multiplicity (number of pmts in Milagro which detect light) events which are typically low primary energy EAS. It is also maximal for EAS whose cores land far from the pond.

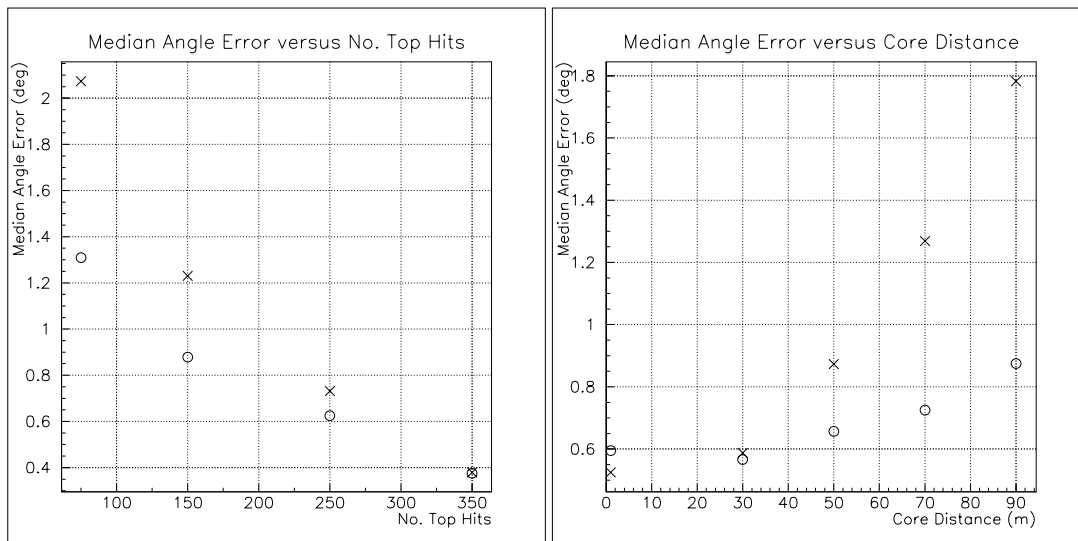


Figure 3: Plots of median angle error versus number of pmt hits in top layer of Milagro pond and versus EAS core distance from center of Milagro pond. Circles are values when tanks are used and crosses are value when tanks are not used.

3.2 Improvements in Trigger Sensitivity Including tank acquired information within the Milagro trigger condition can increase the efficiency for seeing low energy events. This is clearly seen in Figure 4 which displays a plot of the effective area of the Milagro detector for three types of triggers. The pond-only trigger is a requirement that at least 50 pmts be hit by the EAS. The tank+pond trigger is that either the pond trigger be satisfied or that at least 5 tanks be hit by the EAS. The tank-only trigger is that at least 5 tanks be hit and that less than 50 pond pmts be hit by the EAS. The tank-only trigger is included to explicitly show the contribution of the tanks to the effective area.

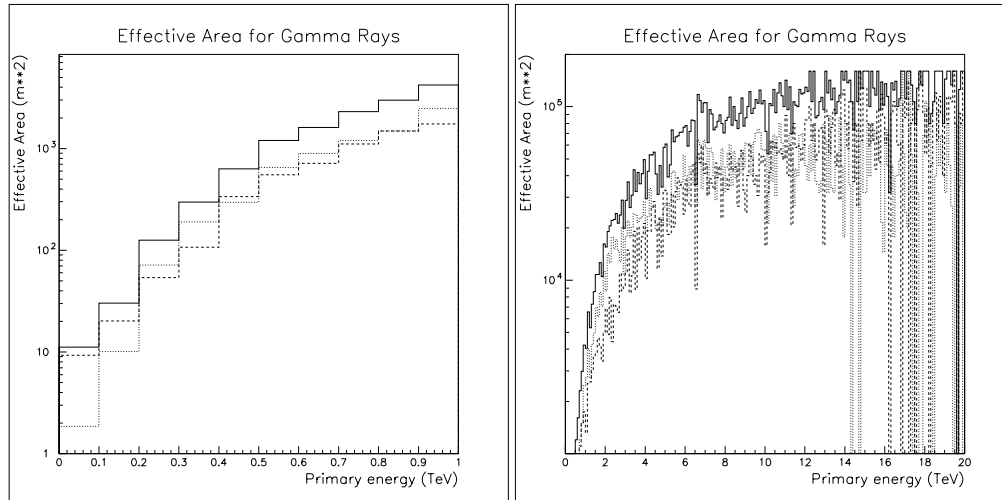


Figure 4: Plot of effective area versus energy. Dashed is pond-only trigger, dotted is tank-only trigger, and solid is pond-tank trigger.

Those events obtained by using the tanks in a trigger condition have an average pond pmt multiplicity of 20 and an angular resolution of about 2.5° . This resolution is significantly worse than the resolution of pond-triggered events ($< 1.0^\circ$) but is adequate for doing coincident searches with most BATSE-detected Gamma Ray Bursts and for photon counting analyses where the event angles are not used.

4 Results from a Prototype Array

A prototype tank array has been installed near the Milagro pond to study the response of the water tanks to typical EAS that trigger Milagro. The array consists of 11 tanks built with commercially available polyethylene storage tanks. The installed pmts are of the same type as those in the Milagro pond (Hamamatsu R5912). The tanks are at various distances from the pond which will enable us to study their response as a function of EAS core distance and particle density. The tank hit multiplicity with at pond trigger requirement of approximately 120 hit pond pmts is 2.5. Results from these prototypes will also be presented.

5 Summary

From the above simulation results one can see the predicted large improvement to both the angular and core position resolutions of the Milagro detector using information acquired by a spare array of instrumented Cherenkov water tanks. This improvement is mainly for EAS whose cores do not fall directly on the Milagro pond. Since the sensitivity of an VHE detector is proportional to its angular precision, this improvement will have a large positive effect on Milagro's sensitivity. The greatly improved core position resolution will increase Milagro's sensitivity to various source spectral characteristics.

This research was supported in part by the National Science Foundation, the U. S. Department of Energy Office of High Energy Physics, the U. S. Department of Energy Office of Nuclear Physics, Los Alamos National Laboratory, the University of California, the Institute of Geophysics and Planetary Physics, The Research Corporation, and CalSpace.

References

- McCullough, J.F. 1999, HE 6.1.02, these ICRC proceedings.
 Westerhoff et al. 1998, 19th Texas Symposium on Relativistic Astrophysics proceedings.
 Yodh, G.B. 1996, Space Science Reviews, **75**: 199-212.

Detection of 6 November 1997 Ground Level Event by Milagrito

J.M. Ryan¹ for Milagro collaboration

¹Space Science Center, University of New Hampshire, Durham, NH 03824 USA

Abstract

Solar Energetic Particles from the 6 November 1997 solar flare/CME (coronal mass ejection) with energies exceeding 10 GeV have been detected by Milagrito, a prototype of the Milagro Gamma Ray Observatory. While particle acceleration beyond 1 GeV at the Sun is well established, few data exist for protons or ions beyond 10 GeV. The Milagro observatory, a ground based water Cherenkov detector designed for observing very high energy gamma ray sources, can also be used to study the Sun. Milagrito, which operated for approximately one year in 1997/98, was sensitive to solar proton and neutron fluxes above ~5-10 GeV. Milagrito operated in a scaler mode, which was primarily sensitive to muons, low energy photons, and electrons, and the detector operated in a mode sensitive to showers and high zenith angle muons. In its scaler mode, Milagrito registered a rate increase coincident with the 6 November 1997 ground level event observed by Climax and other neutron monitors. A preliminary analysis suggests the presence of >10 GeV particles.

1 Introduction:

Particle acceleration beyond 1 GeV at the Sun is well established (Parker, 1957), but its intensity and energy still amazes researchers. However, few data exist demonstrating acceleration of protons or ions beyond 10 GeV (Chiba et al., 1992; Karpov et al., 1997; Lovell et al., 1998). The energy upper limit of solar particle acceleration is unknown but is an important parameter, since it relates not only to the nature of the acceleration process, itself not ascertained, but also to the environment at or near the Sun where the acceleration takes place. The Milagro instrument, a water Cherenkov detector near Los Alamos, NM, is at 2650 m elevation with a geomagnetic cutoff rigidity of ≈ 3.5 GV. It is sensitive to solar hadronic cosmic rays from approximately 5 GeV to beyond 1 TeV. These primary particles are detected via Cherenkov light, produced by the secondary shower particles, as they traverse a large ($80 \times 60 \times 8$ m) water-filled pond containing 723 photomultiplier tubes (228 PMTs for the prototype, Milagrito). This energy range overlaps that of neutron monitors (< 10 GeV) such that Milagro complements the worldwide network of these instruments. These ground based instruments, in turn, complement spacecraft cosmic ray measurements at lower energies. This suite of instruments may then be capable of measuring the full energy range of solar hadronic cosmic rays, with the goal of establishing a fundamental upper limit to the efficiency of the particle acceleration by the Sun.

Milagro's baseline mode (air shower telescope mode) of operation measures extensive air showers above 300 GeV from either hadrons or gamma rays. A description of Milagro's capabilities as a VHE gamma ray observatory is available elsewhere in these proceedings (McCullough, 1999). Milagro measures not only the rate of these events but also the incident direction of each event, thereby localizing sources. While performing these measurements, the instrument records the rate of photomultiplier hits (the scaler mode), with an intrinsic energy threshold of about 5 GeV for the progenitor cosmic ray to produce at least one hit. The scaler mode is similar to that of a neutron monitor, while the telescope mode can significantly reduce background by pointing. With a proposed fast data acquisition system (DAQ) and modified algorithms for determining incident directions of muons, the energy threshold of Milagro's telescope mode will be reduced

to ~10 GeV by detecting the (≈ 300 kHz) single muons and mini muon showers. For now, this low energy threshold can only be achieved by using Milagro in the scaler mode, which is not capable of localizing sources. A description of the Milagro solar telescope mode was presented earlier (Falcone et al., 1999).

2 Solar Milagro/Milagrito Scaler Mode:

In scaler mode, a substantial portion of the rate recorded by Milagro (and Milagrigo) is due to muons, and an integral measurement above threshold is performed. These data will provide an excellent high energy complement to the network of neutron monitors, which has been, and continues to be, a major contributor to our understanding of solar energetic particle acceleration and cosmic rays. Monte Carlo events have been used to estimate the effective areas of Milagrigo to protons incident on the atmosphere isotropically, at zenith angles ranging from 0° - 60° (see figure 1). The effective area curves for Milagro, which have been plotted for the sake of comparison, are for vertically incident protons. At 10 GeV, Milagro's scaler mode has nearly 100 times the effective area of a neutron monitor, with the effective area rising rapidly with energy, while Milagrigo had approximately 4 times the effective area of a neutron monitor at 10 GeV. Pressure, temperature, and other diurnal corrections must be applied to the ground level scaler rate (Hayakawa, 1969). We have begun to determine these correction factors for Milagro/Milagrito, and we find them to be reasonably consistent with past work with muon telescopes (Fowler & Wolfendale, 1961). However, these corrections are less important for transient (i.e. solar) events that rise above background quickly and have short durations.

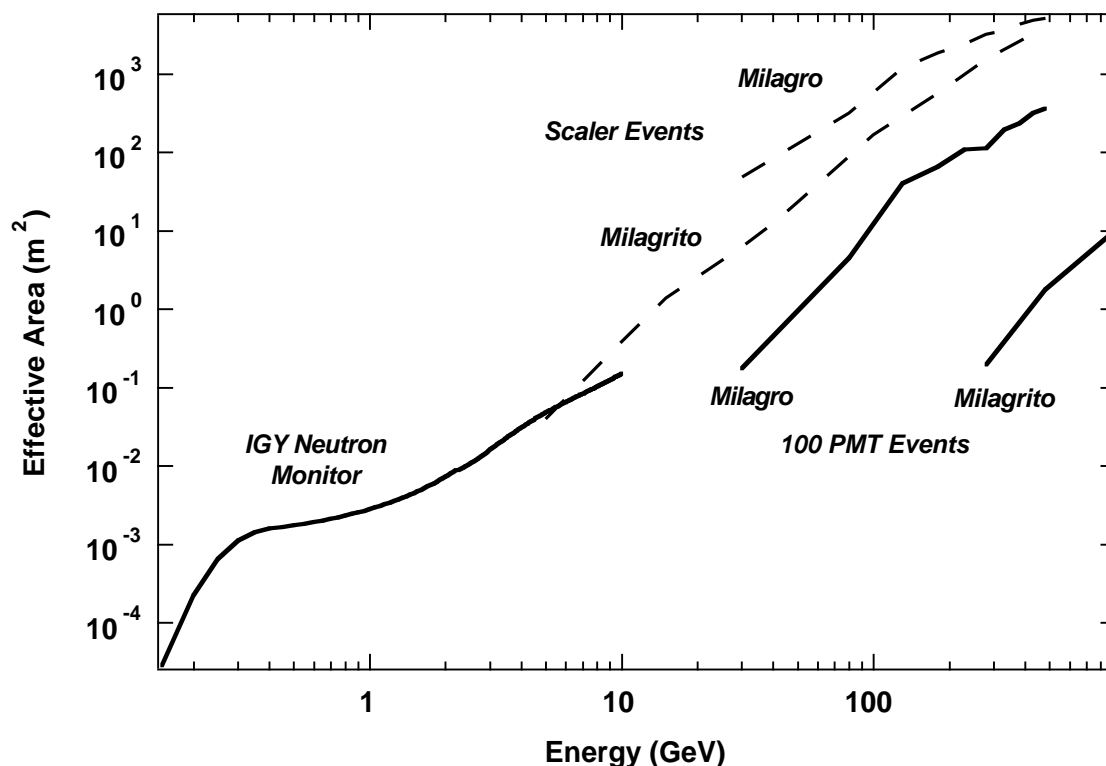


Figure 1 : Effective area curves for Milagro and Milagrigo, with an IGY neutron monitor for comparison.

(Milagro shower trigger presently requires ≈ 150 PMTs)

3 November 6, 1997 Ground Level Event:

On 6 November 1997 at approximately 12:00 UT, an X-class flare with an associated coronal mass ejection occurred on the Sun. This produced a nearly isotropic ground level event registered by many neutron monitors. A preliminary analysis of neutron monitor data for this proton event yields the spectral index of 5.5 at event maximum, assuming a power law proton spectrum (Smart & Shea, 1998). Climax, located in nearby central Colorado, is the closest of these neutron monitors to Milagro/Milagrito. Milagrito, a prototype version of Milagro with less effective area, registered a scaler rate increase coincident, within error, with that measured by Climax (see Figure 2). If one accounts for the meteorological fluctuations, the event duration and time of maximum intensity, as seen by Milagrito, are also consistent with that of Climax.

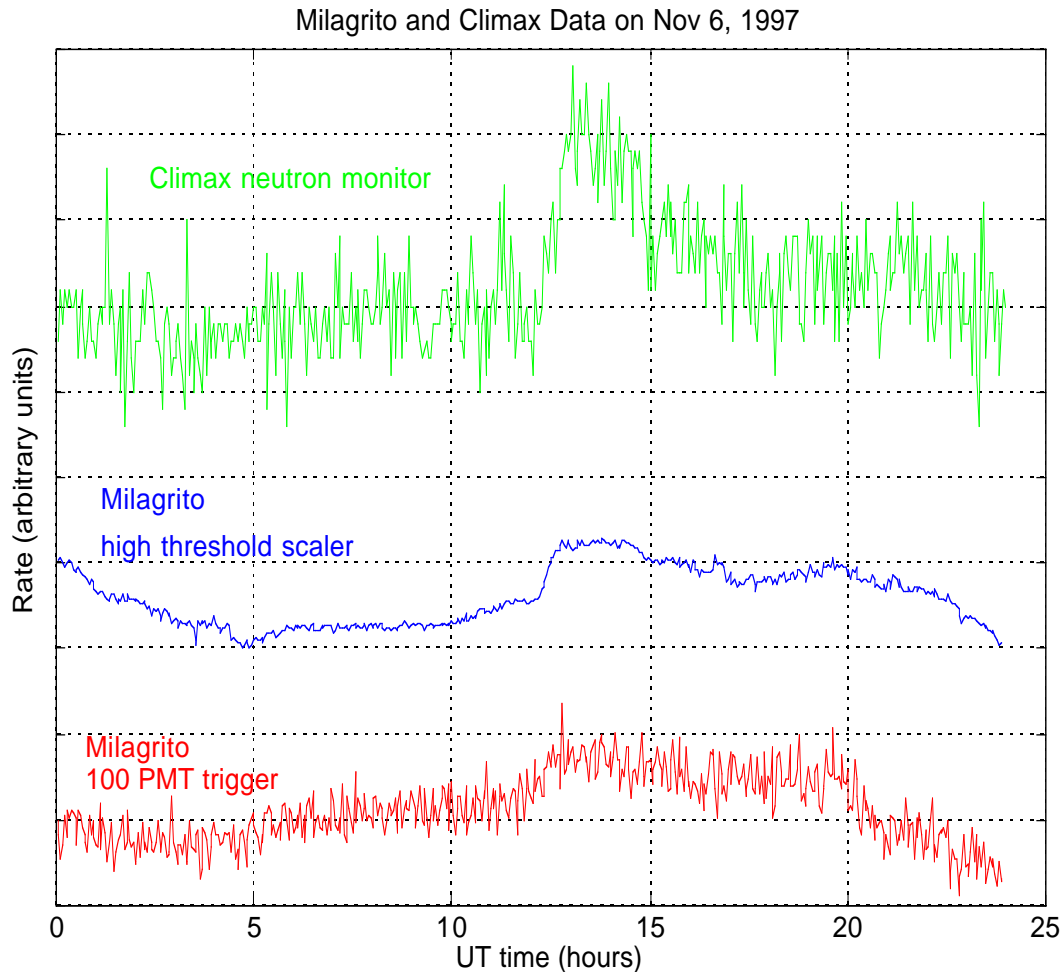


Figure 2 : Milagrito registered a rate increase coincident with that of Climax during the GLE of Nov. 6, 1997. The y-axis units have been scaled and shifted for each plot to make comparison easier. (Climax data courtesy of C. Lopate, Univ. of Chicago)

The 100 PMT shower trigger rate also experienced an increase, although the significance is not as great as that in scaler mode. It is not yet clear which of several possible mechanisms initiated the signal in the 100 PMT shower trigger. This increase can be caused by high energy primaries (> 100 GeV, see figure 1) or secondary muons arriving from a nearly horizontal direction. If the signal was caused by high energy protons, then it can be compared to the scaler mode rate increase in order to derive a proton spectrum. This is done by integrating a “test sample” power law spectrum of protons multiplied by the effective area for the detector in its two modes. The parameters of the “test sample” are then varied until a good fit to the measured rate increases is achieved. This analysis was done, using an extrapolated form of the 100 PMT mode effective area curve, and the derived power law spectrum has an index of >7 . This spectrum derived from Milagrito is softer than that of the world wide network of neutron monitors (index ≈ 5.5), likely indicating a cutoff, or a roll over, somewhere in Milagrito’s range of sensitivity. However, it appears as though horizontal secondary muons have contributed to this signal. These muons could still be the result of proton primaries, but the effective area of the detector would be significantly different from that assumed here. Future work will address this issue by recalculating the spectrum by analyzing events caused by horizontally incident secondary muons.

This work is supported in part by the National Science Foundation, U.S. Department of Energy Office of High Energy Physics, U.S. Department of Energy Office of Nuclear Physics, Los Alamos National Laboratory, University of California, Institute of Geophysics and Planetary Physics, the Research Corporation, and the California Space Institute.

4 References:

- Parker, E.N. 1957, *Physical Review* 107 830.
- Chiba, N., et al. 1992, *Astroparticle Physics*, 1(1) 27-32.
- Karpov, S.N., Miroshnichenko, L.I., Vashenyuk, E.V. 1997, *Proc. 25th Int. Cosmic Ray Conf.* 1 205.
- Lovell, J.L., Duldig, M.L., Humble, J.E. 1998, *Journal of Geophysical Research* 103(A10) 23733.
- McCullough, J.F., et al. 1999, *these ICRC proceedings*, HE 6.1.02,
- Falcone, A.D., et al., 1999, (accepted for publication in *Astrop. Phys.*)
- Hayakawa, S. 1969, *Cosmic Ray Physics* (John Wiley and Sons, NY).
- Fowler, G.N., Wolfendale, A.W. 1961, in *Cosmic Rays I* S.Flügge, eds. 312.
- Smart, D.F & Shea, M.A. 1998, *Proc. Spring American Geophysical Union Meeting*

Study of the Shadow of the Moon and Sun with VHE Cosmic Rays

M.O. Wascko¹

¹*Department of Physics, University of California, Riverside, Riverside, CA 92521, USA*
for the Milagro collaboration

Abstract

Milagrito, a prototype for the Milagro detector, operated for 15 months in 1997-8 and collected 8.9×10^9 events. It was the first extensive air shower (EAS) array sensitive to showers initiated by primaries with energy below 1 TeV. The shadows of the sun and moon observed with cosmic rays can be used to study systematic pointing shifts and measure the angular resolution of EAS arrays. Below a few TeV, the paths of cosmic rays coming toward the earth are bent by the helio- and geo-magnetic fields. This is expected to distort and displace the shadows of the sun and the moon. The moon shadow, offset from the nominal (undeflected) position, has been observed with high statistical significance in Milagro. This can be used to establish energy calibrations, as well as to search for the anti-matter content of the VHE cosmic ray flux. The shadow of the sun has also been observed with high significance.

1 Introduction:

Extensive air shower (EAS) arrays have been used to search for astrophysical point sources of ultra high energy (UHE) and very high energy (VHE) γ -rays for decades, from the PeV to EeV regions in the 70's, down to 10 TeV in the 90's. To distinguish a point source of γ -rays from the large isotropic background of cosmic ray protons and nuclei, a detector must have at least one of the following two capabilities: it must be capable of distinguishing between photon and hadron initiated showers, or it must have angular resolution sharp enough to detect a significant excess of events above the isotropic cosmic ray flux. Typically, hadron-initiated showers have higher muon content than photon initiated showers, but at lower energies this difference is not as striking. Thus in the VHE region, angular resolution is a critical parameter for detector performance, regardless of particle identification capabilities.

As they pass overhead during a transit, the moon and the sun block cosmic rays, so their shadows in the cosmic ray flux should be visible to EAS arrays with sufficiently good angular resolution (Clark, 1957). A detector with perfect angular resolution would see a sharp bucket shaped deficit of events of radius 0.26° centered at the expected position of the moon or sun. In reality, the deficit of events is spread out from the expected position due to finite angular resolution effects. It is thus possible to use the observed shadows of the moon and the sun in the cosmic ray flux to determine the angular resolution of an EAS detector (Alexandreas, et al. 1991). By comparing the observed position of the deficit to the expected position, the shadowing effect can be used to determine whether there are systematic pointing shifts (Alexandreas, et al. 1991).

In the TeV regime, the paths of charged cosmic rays are noticeably bent by the magnetic fields of the earth and the sun. Thus it is expected that the shadows of the moon and the sun will be offset from their nominal positions. The amount of the magnetic deflection varies with the rigidity, $\frac{|p|}{Z}$, of the primary particle, as well as the magnitude and direction of the magnetic field. Cosmic rays approaching the earth from different directions sample different parts of the geomagnetic field, and the effects of the magnetic deflection on the moon's shadow will differ. The sun's shadow should be somewhat more dispersed than the moon's shadow due to the complexity and variability of the heliomagnetic field (Amenomori et al. 1993). The sun's magnetic field changes noticeably in magnitude on time scales of several years.

By studying the effects of the geomagnetic deflection on the moon shadow, especially as a function of incident angle, it is possible to gain some understanding of the energy response of the detector. Lower energy particles will be deflected more than higher energy particles, and this will smear the shape of the shadow in

addition to deflecting its position. Energy resolution is traditionally one of the weaker aspects of EAS arrays, and thus the moon's shadow again offers itself as a useful tool for understanding the detector's capabilities. The effect of the magnetic field can also be used to search for the antiproton to proton ratio in the VHE cosmic ray flux, since negatively charged antiprotons would be bent in the opposite direction that positively charged protons would be bent (Urban et al. 1990).

2 Experimental Technique

Milagrito was the prototype stage of the Milagro Gamma Ray Observatory. Consisting of a single layer of upward facing photomultiplier tubes (PMTs) submerged beneath 1-2 meters of water, it operated between February 1997 and May 1998 and collected 8.9×10^9 air shower events (Atkins, et al., 1999). Simulations indicate that Milagro is capable of detecting showers from primaries with energies as low as 100 GeV, with the median energy of detected showers varying as a function of zenith angle. The present analysis is based on the subset of events whose arrival direction was within 8° of the moon's direction.

The methods used to extract the angular resolution and the systematic pointing shifts from the moon's shadow have been developed previously (Alexandreas, et al., 1991, Amenomori, et al., 1993). The event density as a function of the angular separation from the moon's position is calculated, and the shape of the deficit of events is analyzed using the maximum likelihood method. This assumes *a priori* knowledge of the shape of the resolution function; typically a two dimensional Gaussian (Alexandreas, et al., 1991), or a sum of two dimensional Gaussians (Amenomori, et al., 1993), is assumed. This analysis can yield both the most probable value for the width of the Gaussian point spread function, and the most probable position of the center of the deficit. The first result is the angular resolution of the detector, and the second gives the systematic pointing shift.

At TeV energies this is complicated by the fact that the position of maximum deficit is *expected* to be offset from the nominal position of the moon, due to the geomagnetic deflection. Thus a careful simulation study of the effects of the geomagnetic field is required. The same is true of the shadow of the sun.

3 Simulations

The Monte Carlo simulations of air showers and the detector are described elsewhere (Atkins, et al. 1999). A systematic pointing error in Milagro was identified with the detector simulations. The effect is that air showers are reconstructed with zenith angles systematically closer to the horizon than the incident directions of the primary particles. This is thought to stem primarily from late light traveling laterally across the pond. The effect

Moon Shadow Significance

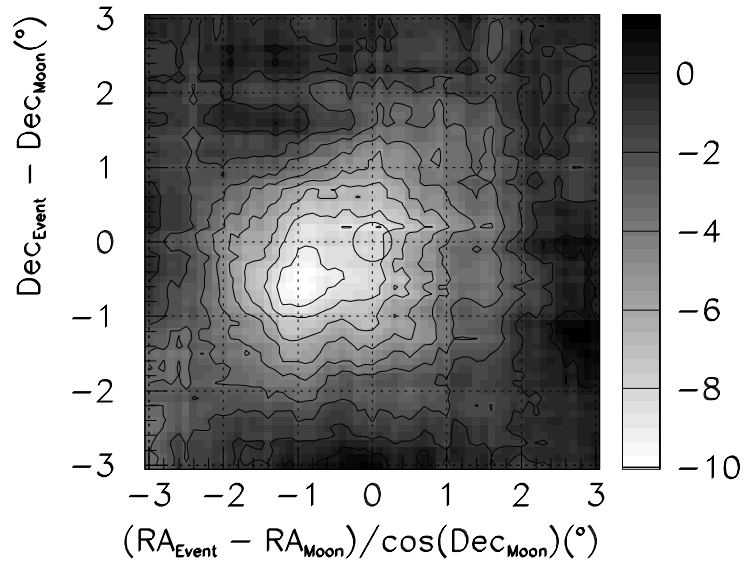


Figure 1: Two dimensional plot of the moon shadow. The background was calculated using the time-slicing method (Alexandreas et al., 1993). The data and background maps were then smoothed with square bins 2.1° on a side. The significance was calculated by the method of Li & Ma (Li & Ma, 1983). The circle shown is of radius 0.26° and is centered at the undeflected position of the moon.

was removed from Milagro with the addition of reflective baffles on the PMTs, and the systematic error is not observed in the Milagro detector simulations. Simulations were also run in which cosmic ray primaries of varying rigidities were propagated through the Earth’s magnetic field between the moon and the top of the atmosphere. The geomagnetic field was assumed to be a dipole, with the dipole axis coincident with the true magnetic poles. The angular deflection as a function of rigidity and incident direction was calculated in local detector coordinates and applied to events thrown from the moon as if it were a source of cosmic rays. These moon source events were then subtracted from a sample of separately simulated background events. This simulated moon shadow incorporates the effects of the systematic pointing error already identified with the Monte Carlo as well as the effect of the geomagnetic field. Further discrepancies between the data and the simulation would then indicate an additional systematic pointing shift.

4 Results and Conclusions

Barring systematic pointing shifts, one can make a prediction of the position of the center of the deficit of events, based on the simulations. Using this position as the location of the moon shadow, the event density as a function of angular separation from the moon shadow can be calculated. Unlike previous EAS moon shadow analyses, this calculation yields an upper limit of the angular resolution of Milagrito, rather than the resolution itself. This is because the spread of events in the deficit is due to the combined effects of the geomagnetic deflection and the finite angular resolution of Milagrito. To extract the angular resolution, one must use the simulations to unfold the two effects.

By carefully studying the shape of the moon shadow, one may be able to learn something about the energy response of the detector, since primaries of different rigidities will be deflected by different amounts. This may also lead to an energy calibration of Milagrito.

It is also possible to simulate a shadow of the moon in a flux of anti-matter cosmic rays. By combining such a simulation with the previous simulations, a prediction of the location and magnitude of a moon “anti-shadow”, and then a search for such a feature in the data, can be made. In this way a measurement of the anti-matter content of the VHE cosmic ray flux can be made.

The shadow of the sun has also been observed with Milagrito, and is shown in Figure 2. Analyses of these measurements is in progress, and results will be presented.

5 Acknowledgments

This research was supported in part by the National Science Foundation, the U. S. Department of Energy Office of High Energy Physics, the U. S. Department of Energy Office of Nuclear Physics, Los Alamos National Laboratory, the University of California, and the Institute of Geophysics and Planetary Physics, The Reasearch Corporation, and CalSpace.

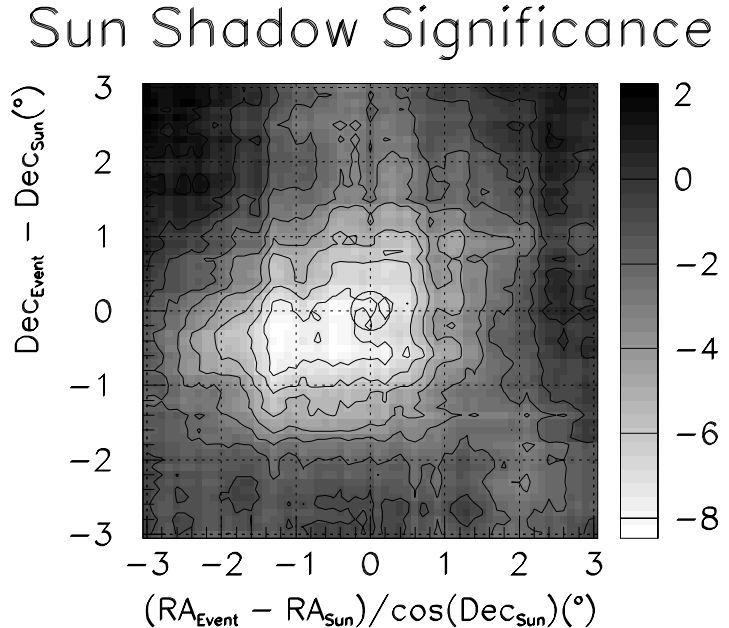


Figure 2: Two dimensional plot of the sun shadow. The background and significance were calculated in the same way as in the moon shadow plot.

References

- Alexandreas, D.E. et al., 1991 Phys. Rev. D43, 1735.
Alexandreas, D.E. et al., 1993 Nucl. Instr. Meth. A328, 570.
Amenomori, M. et al., 1993 Phys. rev. D47, 2675.
Atkins et al. 1999, Nucl. Instr. Meth. A, in preparation.
Clark, G.W., 1957, Phys. Rev. 108, 450.
Li, T.P. & Ma, Y.Q., 1983 ApJ 272, 317.
Urban, M. et al., in *Astrophysics and Particle Physics*, Proceedings of the Topical Seminar, San Miniato, Italy, 1989, edited by G. Castellini et al. [Nucl. Phys. B(Proc. Suppl.), 14B, 223 (1990)].